

Superconductivity in multi-Weyl semimetals: Conditions for the coexistence of topological and conventional phases

Alonso Tapia¹ and Enrique Muñoz  ^{1,2,*}

¹*Facultad de Física, Pontificia Universidad Católica de Chile, Vicuña Mackenna 4860, Santiago, Chile*

²*Center for Nanotechnology and Advanced Materials CIEN-UC,*

Avenida Vicuña Mackenna 4860, Santiago, Chile

(Dated: December 23, 2025)

In this work, we explore the possible emergence of superconducting phases in a multi-Weyl semimetal. In particular, we show that the presence of a pair of Weyl nodes with chirality $|\nu| \geq 1$ leads to an effective description of the intra-nodal pairings in terms of monopole harmonics, in contrast to inter-nodal pairings that preserve the angular dependence of conventional spherical harmonics. Therefore, we explore the conditions for the competition and/or coexistence between both types of superconducting phases, and we identify the presence of the so-called "topological repulsion" mechanism, which was previously reported in the context of simple Weyl semimetals. We identified the critical temperatures corresponding to the monopole and conventional superconducting phases, and calculated the specific heat as a function of temperature, thus showing that this thermodynamical parameter may provide an experimental probe to determine the chirality index ν in the material.

I. INTRODUCTION

Since their theoretical prediction, Weyl semimetals have been studied with great interest^{1–3} due to their unusual properties. The presence of pairs of gapless nodal points connecting the valence and conduction bands leads to different quasiparticle excitations^{4–7}. In single Weyl semimetals (WSMs), the nodal points exhibit nearly linear dispersion where quasiparticles are pseudorelativistic Weyl fermions^{7,8}, as experimentally verified^{9–13} in transition metal monopnictides (TaAs^{14–16}, TaP^{17,18}, NbAs¹⁹ and NbP), and in other materials such as ZrTe₅²⁰ and Cd₃As₂²¹. Each Weyl node is a monopolar source of Berry curvature, and hence they are protected from being gapped since their monopole charge $C = \pm 1$ (chirality) is a topological invariant^{7,8}, thus involving "spin-momentum locking" for Weyl fermions. Among the remarkable properties of these materials are the presence of Fermi arcs, the chiral anomaly, and the chiral magnetic effect^{7,8,22}.

Recently, another type of WSM was proposed, known as multi-Weyl^{23–25}. These materials have multiple Weyl nodes (double or triple) with an anisotropic dispersion relationship that is only linear in one direction, and quadratic or cubic in the other two directions. Therefore, the different chiral charges and the semi-linear dispersion of the electronic bands imply modified spin-momentum locking properties, as well as the possible existence of novel strongly correlated phases in the presence of interactions^{26–29}. Examples of candidate materials are SrSi₂^{24,30}, HgCr₂Se₄^{27,31}, RhAs₃³², Rb(MoTe)₃³³ and Tl(MoTe)₃³³.

The topological features of the band structure in WSMs suggest the possible existence of diverse pairing states^{34–38}. In particular, the monopole superconductor (MSC), recently proposed as a pairing state between the two Fermi surfaces (FSs) enclosing the Weyl points in a doped WSM^{37,38}, involves the superposition of the

Berry phases of the individual single-particle states, thus determining the Berry phase of the emerging Cooper pair. Therefore, the resulting chirality, i.e. the vorticity of the pair, will be characterized by the combination of those of the individual Weyl nodes. For spherically symmetric Fermi surfaces, it was shown³⁷ that the pairing will correspond to monopole harmonic functions, in contrast to the spherical harmonics in conventional superconductivity. In order to experimentally detect those non-trivial vorticity effects, magneto-transport measurements can be applied to discriminate chiral versus non-chiral pairing states. This mechanism has been investigated by one of the authors^{39,40} in the context of the competition between the monopole pairing, characterized by the monopole harmonic functions $\mathcal{Y}_{q,j,m}(\theta, \varphi)$, with conventional spherical harmonic states $Y_{j,m}(\theta, \varphi)$. In this previous work, within a mean-field BCS theory, we showed that the monopole and a conventional spherical harmonic phase may coexist with one another^{39,40}, while exclusion of one phase in favor of the other arises when the θ -dependent form factors of the monopole harmonic $\mathcal{Y}_{|q|,j,|m|}(\theta, \varphi)$ and the spherical harmonic $Y_{j,m}(\theta, \varphi)$ are proportional to each other. We termed this mechanism as "topological repulsion"³⁹. In the present work, we extend the theoretical analysis^{39,40} to study the possible emergence of topological superconducting phases, and in particular the competition between conventional and monopole pairing, in the context of multi-Weyl semimetals. Furthermore, we analyze the critical temperatures for each of those phases, and the specific heat as a possible probe for the chirality index ν in multi-WSMs.

II. THE MODEL

Let us start from the general form of the Hamiltonian representing a Weyl semimetal in the presence of particle-

particle interactions

$$\hat{H} = \hat{H}_0 + \hat{V}. \quad (1)$$

Here, the non-interacting contribution is defined, in a generalized two-band model, by

$$\hat{H}_0 = \sum_{\mathbf{k}, \sigma, \sigma'} \hat{c}_{\sigma, \mathbf{k}}^\dagger [\mathbf{N}(\mathbf{k}) \cdot \boldsymbol{\sigma}]_{\sigma \sigma'} \hat{c}_{\sigma', \mathbf{k}}, \quad (2)$$

for fermion operators $[\hat{c}_{\sigma, \mathbf{k}}, \hat{c}_{\sigma', \mathbf{k}'}^\dagger]_+ = \delta_{\mathbf{k}, \mathbf{k}'} \delta_{\sigma, \sigma'}$, with $\boldsymbol{\sigma} = (\hat{\sigma}^x, \hat{\sigma}^y, \hat{\sigma}^z)$ the usual Pauli matrices. The explicit form of the components of the vector $\mathbf{N}(\mathbf{k}) = (N_1(\mathbf{k}), N_2(\mathbf{k}), N_3(\mathbf{k}))^T$ determines the topological properties of the effective two-band model, and the corresponding energy bands are trivially $E_{\mathbf{k}}^\pm = \pm |\mathbf{N}(\mathbf{k})|$. For instance, a double WSM can be realized by⁴¹

$$\begin{aligned} N_1(\mathbf{k}) &= t(\cos k_x - \cos k_y) \\ N_2(\mathbf{k}) &= t \sin k_y \sin k_x \\ N_3(\mathbf{k}) &= t_z \cos(k_z a) - m_z + t_0 \{6 + \cos(2k_x) + \cos(2k_y) \\ &\quad - 4 \cos k_x - 4 \cos k_y\} \end{aligned} \quad (3)$$

In addition, we shall assume a short-range interaction, involving a nearest-neighbors Coulomb repulsion $V_1 > 0$ and a contact, phonon-mediated effective attractive interaction $V_0 < 0$. When both terms are combined we have⁴⁰

$$\hat{V} = V_0 \sum_i \hat{n}_i \hat{n}_i + \frac{1}{2} V_1 \sum_{\langle i, j \rangle} \hat{n}_i \hat{n}_j. \quad (4)$$

Here $\hat{n}_i = \sum_{\sigma} \hat{c}_{\sigma}^\dagger(\mathbf{R}_i) \hat{c}_{\sigma}(\mathbf{R}_i)$ is the occupation number operator at the site \mathbf{R}_i on the lattice in the local Wannier basis. By the appropriate Fourier transformation

$\hat{c}_{\sigma}(\mathbf{R}_i) = \frac{1}{\sqrt{N}} \sum e^{i\mathbf{k} \cdot \mathbf{R}_i} \hat{c}_{\sigma}(\mathbf{k})$, the interaction term is expressed in the Bloch-momentum basis by

$$\hat{V} = \sum_{\mathbf{k}, \mathbf{p}, \mathbf{q}, \sigma, \tau} V_{\mathbf{q}} \hat{c}_{\sigma, \mathbf{k} + \mathbf{q}}^\dagger \hat{c}_{\sigma, \mathbf{k}} \hat{c}_{\tau, \mathbf{p} - \mathbf{q}}^\dagger \hat{c}_{\tau, \mathbf{p}}, \quad (5)$$

with a matrix element given by

$$V_{\mathbf{q}} = V_0 + V_1(\cos q_x + \cos q_y + \cos q_z). \quad (6)$$

In order to capture the topological features of the multi-Weyl semimetal band structure, we define operators in the nodal Fermi surface representation, by expanding the momenta in the vicinity of each Weyl point as follows $\hat{\psi}_{\pm, \sigma}(\mathbf{k}) = \hat{c}_{\sigma}(\mathbf{k} + \mathbf{K}_{\pm})$ for $|\mathbf{k}| \ll |\mathbf{K}_{\pm}|$. In this nodal representation, a generic low-energy model for a multi-Weyl semimetal with topological charge $\nu \in \mathbb{N}$ is⁴¹

$$\begin{aligned} \hat{H}_0 = \sum_{\mathbf{k}, a=\pm} \hat{\psi}_a^\dagger(\mathbf{k}) \{ &v_F [\alpha_{\nu} k_{\perp}^{\nu} \cos(\nu \phi_{\mathbf{k}}) \hat{\sigma}^x \\ &+ \alpha_{\nu} k_{\perp}^{\nu} \sin(\nu \phi_{\mathbf{k}}) \hat{\sigma}^y + a k_z \hat{\sigma}^z] - \mu^a \} \hat{\psi}_a(\mathbf{k}), \end{aligned} \quad (7)$$

where $a = \pm$ represents the sign of the nodal topological charge (chirality), and μ^a is the chemical potential at each node.

For the interaction operator, we take a similar approach, starting from the Bloch-momentum representation (5) and choosing the pairing mechanism of our interest,

$$\hat{V} = \sum_{\mathbf{k}, \mathbf{q}, \mathbf{p}} V_{\mathbf{q}}^{ab, cd} \hat{\psi}_{a, \sigma}^\dagger(\mathbf{k} + \mathbf{q}) \hat{\psi}_{b, \tau}^\dagger(\mathbf{p} - \mathbf{q}) \hat{\psi}_{c, \tau}(\mathbf{p}) \hat{\psi}_{d, \sigma}(\mathbf{k}), \quad (8)$$

where now we include all the interaction coefficients in a single matrix element $V_{\mathbf{q}}^{ab, cd}$. Explicitly, expanding up to second order in the momenta, we obtain⁴⁰

$$\begin{aligned} V_{\mathbf{k}, \mathbf{q}}^{\pm\pm, \pm\pm} &= V_{\mathbf{k}, \mathbf{q}}^{\pm\mp, \mp\pm} = V_0 + V_1 \left(3 - \frac{(\mathbf{k} - \mathbf{q})^2}{2} \right) \\ V_{\mathbf{k}, \mathbf{q}}^{\pm\mp, \pm\mp} &= V_0 + V_1 \left\{ 2 - \frac{|\mathbf{k}_{\perp} - \mathbf{q}_{\perp}|^2}{2} + \left(1 - \frac{(k_z - q_z)^2}{2} \right) \cos 2Q \mp (k_z - q_z) \sin 2Q \right\}, \end{aligned} \quad (9)$$

with $\mathbf{k}_{\perp} = (k_x, k_y, 0)$. The proper treatment of these coefficients in the low-energy regime may lead to the emergence of different superconducting phases, according to their intra- or inter-node pairing structure^{39,40}. In a standard BCS-like mean-field approximation, we write the interaction as

$$\hat{V} = \sum_{\mathbf{k}, \sigma, \tau, a, b} \hat{\psi}_{a, \sigma}^\dagger(\mathbf{k}) \Delta_{\sigma \tau}^{ab}(\mathbf{k}) \hat{\psi}_{b, \tau}^\dagger(-\mathbf{k}) + h.c., \quad (10)$$

where the pairing function is defined via the self-

consistent relation

$$\Delta_{\sigma \tau}^{ab}(\mathbf{k}) = \sum_{\mathbf{q}, c, d} V_{\mathbf{k}, \mathbf{q}}^{ab, cd} \langle \hat{\psi}_{c, \tau}(-\mathbf{q}) \hat{\psi}_{d, \sigma}(\mathbf{q}) \rangle. \quad (11)$$

Following the method presented in³⁹, we introduce the Bogoliubov transformation $\hat{\alpha}_a^\dagger(\mathbf{k}) = \sum_{\sigma} \zeta_{a, \sigma}(\mathbf{k}) \hat{c}_{\sigma, \mathbf{k}}^\dagger(\mathbf{k})$, where the spinor $\zeta_a(\mathbf{k})$ is the positive energy eigenvector of \hat{H}_0 at each Weyl node $a = \pm$. Thus, we have

$$\zeta_{\pm}(\mathbf{k}) = \frac{1}{\sqrt{2\epsilon_{\mathbf{k}}(\epsilon_{\mathbf{k}} \pm k_z)}} \begin{pmatrix} \epsilon_{\mathbf{k}} \pm k_z \\ \alpha_{\nu} k_{\perp}^{\nu} e^{i\nu \phi_{\mathbf{k}}} \end{pmatrix}, \quad (12)$$

where was defined $\epsilon_{\mathbf{k}} \equiv \sqrt{k_z^2 + \alpha_{\nu}^2 k_{\perp}^{2\nu}}$. In this basis, the Hamiltonian is then reduced to

$$\hat{H} = \sum_{\mathbf{k}, a, b} \left\{ \xi_{\mathbf{k}}^a \hat{\alpha}_a^{\dagger}(\mathbf{k}) \hat{\alpha}_a(\mathbf{k}) + \Delta^{ab}(\mathbf{k}) \hat{\alpha}_a^{\dagger}(\mathbf{k}) \hat{\alpha}_b^{\dagger}(-\mathbf{k}) + h.c. \right\}, \quad (13)$$

where the single-particle contribution was diagonalized, leading to the dispersion relation

$$\xi_{\mathbf{k}}^{\pm} = v_F \sqrt{k_z^2 + \alpha_{\nu}^2 k_{\perp}^{2\nu}} - \mu^{\pm}, \quad (14)$$

and the projected gap equation in the new basis becomes

$$\Delta^{ab}(\mathbf{k}) = \sum_{\mathbf{q}, c, d} \bar{V}_{\mathbf{k}, \mathbf{q}}^{ab, cd} \langle \hat{\alpha}_c(-\mathbf{q}) \hat{\alpha}_d(\mathbf{q}) \rangle, \quad (15)$$

with matrix elements $\bar{V}_{\mathbf{k}, \mathbf{q}}^{ab, cd}$ given by the corresponding transformation from the originals to this new basis.

Let us further define the Nambu spinor $\Psi_{\mathbf{k}}^{\dagger} = (\hat{\alpha}_{-}^{\dagger}(\mathbf{k}), \hat{\alpha}_{-}(-\mathbf{k}), \hat{\alpha}_{+}^{\dagger}(\mathbf{k}), \hat{\alpha}_{+}(-\mathbf{k}))$, in order to arrange the Hamiltonian in the Bogoliubov-de Gennes notation as a bilinear form^{39,40}

$$\hat{H} = \sum_{\mathbf{k}} \Psi_{\mathbf{k}}^{\dagger} \hat{H}_{BdG}(\mathbf{k}) \Psi_{\mathbf{k}}, \quad (16)$$

where we defined the matrix

$$\hat{H}_{BdG}(\mathbf{k}) = \begin{pmatrix} \xi_{\mathbf{k}}^{-} & \Delta_{\mathbf{k}}^{\text{intra}} & 0 & \Delta_{\mathbf{k}}^{\text{inter}} \\ (\Delta_{\mathbf{k}}^{\text{intra}})^* & -\xi_{\mathbf{k}}^{-} & (\Delta_{\mathbf{k}}^{\text{inter}})^* & 0 \\ 0 & \Delta_{\mathbf{k}}^{\text{inter}} & \xi_{\mathbf{k}}^{+} & \Delta_{\mathbf{k}}^{\text{intra}} \\ (\Delta_{\mathbf{k}}^{\text{inter}})^* & 0 & (\Delta_{\mathbf{k}}^{\text{intra}})^* & -\xi_{\mathbf{k}}^{+} \end{pmatrix}. \quad (17)$$

For subsequent computations, it is convenient to express this matrix in a $SU(2) \otimes SU(2)$ basis composed by $\{\hat{\tau}_{\alpha} \otimes \hat{\eta}_{\beta}\}$, where $\hat{\tau}_{\alpha}$ span the subspace of the two Weyl nodes, while $\hat{\eta}_{\beta}$ represents the particle-hole degrees of freedom. Here, $\alpha, \beta = 1, 2, 3$ are the Pauli matrix indexes, while $\alpha, \beta = 0$ correspond to the two-dimensional representation of the identity. In this notation, we have

$$\begin{aligned} \hat{H}_{BdG}(\mathbf{k}) &= \bar{\xi}_{\mathbf{k}} \hat{\tau}_0 \otimes \hat{\eta}_3 + \frac{\delta\mu}{2} \hat{\tau}_3 \otimes \hat{\eta}_3 + \Re \Delta_{\mathbf{k}}^{\text{intra}} \hat{\tau}_0 \otimes \hat{\eta}_1 \\ &- \Im \Delta_{\mathbf{k}}^{\text{intra}} \hat{\tau}_0 \otimes \hat{\eta}_2 + \Re \Delta_{\mathbf{k}}^{\text{inter}} \hat{\tau}_1 \otimes \hat{\eta}_1 - \Im \Delta_{\mathbf{k}}^{\text{inter}} \hat{\tau}_1 \otimes \hat{\eta}_2, \end{aligned} \quad (18)$$

where we defined the average chemical potential between the pair of nodes as $\bar{\mu} = (\mu_{+} + \mu_{-})/2$, and the difference by $\delta\mu = \mu_{+} - \mu_{-}$. Accordingly, the single quasiparticle dispersion at the average chemical potential is

$$\bar{\xi}_{\mathbf{k}} = v_F \sqrt{k_z^2 + \alpha_{\nu}^2 k_{\perp}^{2\nu}} - \bar{\mu}. \quad (19)$$

III. THE GAP EQUATIONS

At finite temperature, the field theoretical representation of the partition function is

$$Z = \text{Tr } e^{-\beta \hat{H}} = \int \mathcal{D}\Psi^{\dagger} \mathcal{D}\Psi e^{-\int_0^{\beta} d\tau \sum_{\mathbf{k}} \Psi_{\mathbf{k}}^{\dagger} \left(\frac{\partial}{\partial \tau} + \hat{H}_{BdG} \right) \Psi_{\mathbf{k}}} \quad (20)$$

Therefore, the Green's function matrix in momentum and Matsubara space is defined by

$$\hat{\mathcal{G}}_{\mathbf{k}}(\omega_n) = \left[-i\omega_n + \hat{H}_{BdG}(\mathbf{k}) \right]^{-1}, \quad (21)$$

where $\omega_n = (2n + 1)\pi T$, $n \in \mathbb{Z}$ is the Matsubara frequency for Fermions.

The Green's function is composed by 4 blocks of 2×2 matrices (details in appendix A), as follows

$$\hat{\mathcal{G}}_{\mathbf{k}}(\omega_n) = \begin{pmatrix} \hat{\mathcal{G}}_{\mathbf{k}}^{\text{intra}, -} & \hat{\mathcal{G}}_{\mathbf{k}}^{\text{inter}} \\ (\hat{\mathcal{G}}_{\mathbf{k}}^{\text{inter}})^{\dagger} & \hat{\mathcal{G}}_{\mathbf{k}}^{\text{intra}, +} \end{pmatrix}. \quad (22)$$

Now, we formulate the BCS self-consistent equations, for both the intra-nodal and inter-nodal pairings, as follows

$$\Delta_{\mathbf{k}}^{\text{intra}} = T \sum_{\mathbf{k}', \omega_n} V_{\text{intra}}(\mathbf{k}, \mathbf{k}') \langle \hat{\alpha}_{-}(\mathbf{k}') \hat{\alpha}_{-}(-\mathbf{k}') \rangle \quad (23)$$

$$\Delta_{\mathbf{k}}^{\text{inter}} = T \sum_{\mathbf{k}', \omega_n} V_{\text{inter}}(\mathbf{k}, \mathbf{k}') \langle \hat{\alpha}_{-}(\mathbf{k}') \hat{\alpha}_{+}(-\mathbf{k}') \rangle. \quad (24)$$

The correlation functions involved in the definitions above can be directly obtained from the matrix elements of the Green's function, as follows

$$\begin{aligned} \langle \hat{\alpha}_{-}(\mathbf{k}) \hat{\alpha}_{-}(-\mathbf{k}) \rangle &= [\hat{\mathcal{G}}_{\mathbf{k}}^{\text{intra}, -}]_{12} \\ &= \frac{\Delta_{\mathbf{k}}^{\text{intra}}(E_{\mathbf{k}}^2 - \delta\mu \bar{\xi}_{\mathbf{k}}) - 2\Delta_{\mathbf{k}}^{\text{inter}} B_{\mathbf{k}}}{E_{\mathbf{k}}^4 - 4B_{\mathbf{k}}^2 - \delta\mu^2(\bar{\xi}_{\mathbf{k}}^2 + |\Delta_{\mathbf{k}}^{\text{inter}}|^2)} \end{aligned} \quad (25)$$

$$\langle \hat{\alpha}_{-}(\mathbf{k}) \hat{\alpha}_{+}(-\mathbf{k}) \rangle = [\hat{\mathcal{G}}_{\mathbf{k}}^{\text{inter}}]_{12} \quad (26)$$

$$= \frac{\Delta_{\mathbf{k}}^{\text{inter}}(E_{\mathbf{k}}^2 - \frac{\delta\mu^2}{2}) - 2\Delta_{\mathbf{k}}^{\text{intra}} B_{\mathbf{k}} - i\omega_n \delta\mu \Delta_{\mathbf{k}}^{\text{inter}}}{E_{\mathbf{k}}^4 - 4B_{\mathbf{k}}^2 - \delta\mu^2(\bar{\xi}_{\mathbf{k}}^2 + |\Delta_{\mathbf{k}}^{\text{inter}}|^2)}$$

with

$$E_{\mathbf{k}} = \sqrt{\bar{\xi}_{\mathbf{k}}^2 + |\Delta_{\mathbf{k}}^{\text{intra}}|^2 + |\Delta_{\mathbf{k}}^{\text{inter}}|^2 + \frac{\delta\mu^2}{4} + \omega_n^2} \quad (27)$$

$$B_{\mathbf{k}} = \Re \Delta_{\mathbf{k}}^{\text{intra}} \Re \Delta_{\mathbf{k}}^{\text{inter}} + \Im \Delta_{\mathbf{k}}^{\text{intra}} \Im \Delta_{\mathbf{k}}^{\text{inter}} \quad (28)$$

Then, we perform the sum over Matsubara frequencies ω_n in the gap equations (details in appendix B), to obtain the self-consistent expressions

$$\Delta_{\mathbf{k}}^{\text{intra}} = \frac{1}{2} \sum_{\mathbf{k}'} V_{\text{intra}}(\mathbf{k}, \mathbf{k}') \left[\left(\Delta_{\mathbf{k}'}^{\text{intra}} + \frac{2\Delta_{\mathbf{k}'}^{\text{inter}} B_{\mathbf{k}'} + \delta\mu \bar{\xi}_{\mathbf{k}'} \Delta_{\mathbf{k}'}^{\text{intra}}}{\sqrt{4B_{\mathbf{k}'}^2 + \delta\mu^2(\bar{\xi}_{\mathbf{k}'}^2 + |\Delta_{\mathbf{k}'}^{\text{inter}}|^2)}} \right) \frac{\tanh(\beta\Gamma_{\mathbf{k}'}/2)}{\Gamma_{\mathbf{k}'}} \right. \\ \left. + \left(\Delta_{\mathbf{k}'}^{\text{intra}} - \frac{2\Delta_{\mathbf{k}'}^{\text{inter}} B_{\mathbf{k}'} + \delta\mu \bar{\xi}_{\mathbf{k}'} \Delta_{\mathbf{k}'}^{\text{intra}}}{\sqrt{4B_{\mathbf{k}'}^2 + \delta\mu^2(\bar{\xi}_{\mathbf{k}'}^2 + |\Delta_{\mathbf{k}'}^{\text{inter}}|^2)}} \right) \frac{\tanh(\beta\gamma_{\mathbf{k}'}/2)}{\gamma_{\mathbf{k}'}} \right] \quad (29)$$

$$\Delta_{\mathbf{k}}^{\text{inter}} = \frac{1}{2} \sum_{\mathbf{k}'} V_{\text{inter}}(\mathbf{k}, \mathbf{k}') \left[\left(\Delta_{\mathbf{k}'}^{\text{inter}} + \frac{2\Delta_{\mathbf{k}'}^{\text{intra}} B_{\mathbf{k}'} + \frac{\delta\mu^2}{2} \Delta_{\mathbf{k}'}^{\text{inter}}}{\sqrt{4B_{\mathbf{k}'}^2 + \delta\mu^2(\bar{\xi}_{\mathbf{k}'}^2 + |\Delta_{\mathbf{k}'}^{\text{inter}}|^2)}} \right) \frac{\tanh(\beta\Gamma_{\mathbf{k}'}/2)}{\Gamma_{\mathbf{k}'}} \right. \\ \left. + \left(\Delta_{\mathbf{k}'}^{\text{inter}} - \frac{2\Delta_{\mathbf{k}'}^{\text{intra}} B_{\mathbf{k}'} + \frac{\delta\mu^2}{2} \Delta_{\mathbf{k}'}^{\text{inter}}}{\sqrt{4B_{\mathbf{k}'}^2 + \delta\mu^2(\bar{\xi}_{\mathbf{k}'}^2 + |\Delta_{\mathbf{k}'}^{\text{inter}}|^2)}} \right) \frac{\tanh(\beta\gamma_{\mathbf{k}'}/2)}{\gamma_{\mathbf{k}'}} \right], \quad (30)$$

where were defined

$$\Gamma_{\mathbf{k}}^2 = \bar{\xi}_{\mathbf{k}}^2 + |\Delta_{\mathbf{k}}^{\text{intra}}|^2 + |\Delta_{\mathbf{k}}^{\text{inter}}|^2 + \frac{\delta\mu^2}{4} \\ + \sqrt{4B_{\mathbf{k}}^2 + \delta\mu^2(\bar{\xi}_{\mathbf{k}}^2 + |\Delta_{\mathbf{k}}^{\text{inter}}|^2)}, \quad (31)$$

$$\gamma_{\mathbf{k}}^2 = \bar{\xi}_{\mathbf{k}}^2 + |\Delta_{\mathbf{k}}^{\text{intra}}|^2 + |\Delta_{\mathbf{k}}^{\text{inter}}|^2 + \frac{\delta\mu^2}{4} \\ - \sqrt{4B_{\mathbf{k}}^2 + \delta\mu^2(\bar{\xi}_{\mathbf{k}}^2 + |\Delta_{\mathbf{k}}^{\text{inter}}|^2)}. \quad (32)$$

IV. THE ZERO TEMPERATURE LIMIT

We shall study the competition between both pairings, and therefore the corresponding superconducting phases in the zero temperature limit $T \rightarrow 0$. For small values of $|\Delta_{\mathbf{k}}^{\text{intra}}|$ and $|\Delta_{\mathbf{k}}^{\text{inter}}|$, and assuming that the chemical potential is nearly symmetrical at both nodes $|\delta\mu/\bar{\mu}| \ll 1$, the gap equations reduce to

$$\Delta_{\mathbf{k}}^{\eta} = \frac{1}{2} \sum_{\mathbf{k}'} V_{\eta}(\mathbf{k}, \mathbf{k}') \Delta_{\mathbf{k}'}^{\eta} \left(\frac{1}{\Gamma_{\mathbf{k}'}} + \frac{1}{\gamma_{\mathbf{k}'}} \right), \quad (33)$$

where $\eta = \text{intra}/\text{inter}$.

We shall assume the following angular dependence on the interaction potentials^{39,40}

$$V_{\text{intra}}(\mathbf{k}, \mathbf{k}') = V_{0}^{\text{intra}} Y_{l, m'}(\theta_{\mathbf{k}}, \phi_{\mathbf{k}}) Y_{l, m'}^{*}(\theta_{\mathbf{k}'}, \phi_{\mathbf{k}'}), \\ V_{\text{inter}}(\mathbf{k}, \mathbf{k}') = V_{0}^{\text{inter}} \mathcal{Y}_{\nu, j, m}(\theta_{\mathbf{k}}, \phi_{\mathbf{k}}) \mathcal{Y}_{\nu, j, m}^{*}(\theta_{\mathbf{k}'}, \phi_{\mathbf{k}'}), \quad (34)$$

where

$$A_{\pm} = \Delta_{l, m'}^2 f_{\text{intra}}^2(\theta_x) \pm \bar{\Delta}_{\nu}^2 f_{\text{inter}}^2(\theta_x). \quad (40)$$

with $Y_{l, m}(\theta_{\mathbf{k}}, \phi_{\mathbf{k}})$ and $\mathcal{Y}_{\nu, j, m}(\theta_{\mathbf{k}}, \phi_{\mathbf{k}})$ the conventional spherical and monopole harmonics, respectively. These angular dependencies are consequently inherited by the pairing functions,

$$\Delta_{\mathbf{k}}^{\text{intra}} = \Delta_{l, m'} Y_{l, m'}(\theta_{\mathbf{k}}, \phi_{\mathbf{k}}) = \Delta_{l, m'} f_{\text{intra}}(\theta_{\mathbf{k}}) e^{im' \phi_{\mathbf{k}}} \\ \Delta_{\mathbf{k}}^{\text{inter}} = \bar{\Delta}_{\nu} \mathcal{Y}_{\nu, j, m}(\theta_{\mathbf{k}}, \phi_{\mathbf{k}}) = \bar{\Delta}_{\nu} f_{\text{inter}}(\theta_{\mathbf{k}}) e^{i(m+\nu) \phi_{\mathbf{k}}}. \quad (35)$$

Inserting these expressions into Eq. (33), we get

$$\frac{1}{V_0^{\eta}} = \frac{1}{2} \sum_{\mathbf{k}} |f_{\eta}(\theta_{\mathbf{k}})|^2 \left(\frac{1}{\Gamma_{\mathbf{k}}} + \frac{1}{\gamma_{\mathbf{k}}} \right). \quad (36)$$

Going to the continuum limit, and defining the density of states $\rho(\xi) = \int \frac{d^3 k}{(2\pi)^3} \delta(\xi - \xi_{\mathbf{k}})$ (details in Appendix C), we obtain the expressions

$$\frac{1}{\lambda_{\eta}} = \frac{1}{2B_{\nu}} \int_0^1 \frac{dx x}{\sqrt{1-x^{2\nu}}} \int_0^{2\pi} \frac{d\phi}{2\pi} |f_{\eta}(\theta_x)|^2 \\ \times \int_{-\omega_D}^{\omega_D} d\xi \left(\frac{1}{\Gamma_{\mathbf{k}}} + \frac{1}{\gamma_{\mathbf{k}}} \right), \quad (37)$$

where the effective couplings were defined as $\lambda_{\eta} = \rho(0)V_0^{\eta}$, with $\rho(0)$ the density of states function at the Fermi level. The coefficient $B_{\nu} = \beta(\frac{1}{\nu}, \frac{1}{2})/(2\nu)$ defined in terms of the Beta function, and θ_x is defined according to the expression

$$\tan \theta_x = \frac{cx}{\sqrt{1-x^{2\nu}}}, \quad (38)$$

with the constant $c = \alpha^{-1/\nu} (\mu/v_F)^{1/\nu-1}$.

By further performing the integral in ξ , we end up with

$$\frac{1}{\lambda_{\eta}} = \frac{1}{B_{\nu}} \int_0^1 \frac{dx x}{\sqrt{1-x^{2\nu}}} |f_{\eta}(\theta_x)|^2 \int_0^{2\pi} \frac{d\phi}{2\pi} \left[2 \ln(2\omega_D) - \frac{1}{2} \sum_{s=\pm} \ln(A_{\pm} + 2sB_{\mathbf{k}}) \right], \quad (39)$$

Noting that

$$2B_{\mathbf{k}} = 2\Delta_{l, m'} \bar{\Delta}_{\nu} f_{\text{intra}}(\theta_x) f_{\text{inter}}(\theta_x) \cos[(m' - m - \nu)\phi] \\ \equiv B \cos(r\phi), \quad (41)$$

the integral in ϕ must be solved in different ways depend-

ing on the cases $m' = m + \nu$ or $m' \neq m + \nu$, respectively.

For Case 1: $m' = m + \nu$, we have

$$\frac{1}{2} \int_0^{2\pi} \frac{d\phi}{2\pi} \sum_{s=\pm} \ln(A_+ + 2sB_{\mathbf{k}}) = \frac{1}{2} \sum_{s=\pm} \ln(A_+ + sB) = \frac{1}{2} \ln(A_+^2 - B^2) = \ln(|A_-|), \quad (42)$$

and then we obtain

$$\frac{1}{\lambda_{\eta}} = \frac{1}{B_{\nu}} \int_0^1 \frac{dxx}{\sqrt{1-x^{2\nu}}} |f_{\eta}(\theta_x)|^2 \ln \left[\frac{4\omega_D^2}{|\Delta_{l,m'}^2 f_{\text{intra}}^2(\theta_x) - \bar{\Delta}_{\nu}^2 f_{\text{inter}}^2(\theta_x)|} \right]. \quad (43)$$

On the other hand, for Case 2: $m' \neq m + \nu$, we solve

$$\begin{aligned} \int_0^{2\pi} \frac{d\phi}{2\pi} \ln [A_+ \pm B \cos(r\phi)] &= \sum_{n=1}^r \int_{2\pi(n-1)/r}^{2\pi n/r} \frac{d\phi}{2\pi} \ln [A_+ \pm B \cos(r\phi)] = \frac{1}{r} \sum_{n=1}^r \int_{2\pi(n-1)}^{2\pi n} \frac{d\phi'}{2\pi} \ln (A_+ \pm B \cos \phi') \\ &= \int_0^{2\pi} \frac{d\phi'}{2\pi} \ln (A_+ \pm B \cos \phi') = \ln \left[\frac{1}{2} \left(A_+ + \sqrt{A_+^2 - B^2} \right) \right] = \ln \left[\frac{1}{2} (A_+ + |A_-|) \right], \end{aligned} \quad (44)$$

and then we obtain

$$\frac{1}{\lambda_{\eta}} = \frac{1}{B_{\nu}} \int_0^1 \frac{dxx}{\sqrt{1-x^{2\nu}}} |f_{\eta}(\theta_x)|^2 \left\{ 2 \ln(2\omega_D) - \ln \left[\frac{1}{2} (A_+ + |A_-|) \right] \right\}. \quad (45)$$

A. Topological Repulsion

Let us now examine whether the mechanism that we call "topological repulsion"³⁹ arises in the case of multi-Weyl semimetals as well, according to our present model. Consider Case 1: $m' = m + \nu$, corresponding to Eq. (43), and further assume that $f_{\text{intra}}(\theta_x) \approx f_{\text{inter}}(\theta_x)$. Then, we have

$$\begin{aligned} \frac{1}{\lambda_{\eta}} &= \frac{1}{B_{\nu}} \int_0^1 \frac{dxx}{\sqrt{1-x^{2\nu}}} |f_{\text{intra}}(\theta_x)|^2 \\ &\times \ln \left[\frac{4\omega_D^2}{f_{\text{intra}}^2(\theta_x) |\Delta_{l,m'}^2 - \bar{\Delta}_{\nu}^2|} \right]. \end{aligned} \quad (46)$$

This equation is analogous to the one obtained in³⁹, but here we extend it to multi-Weyl semimetals. Since the right-hand side is the same for $\eta = \text{intra}$ and $\eta = \text{inter}$, we conclude that the phase boundary occurs precisely at $\lambda_{\text{intra}} = \lambda_{\text{inter}}$, thus leaving no room for coexistence in the phase diagram. This is precisely the topological repulsion mechanism already described in³⁹ for simple Weyl semimetals.

B. s-wave vs Monopole

Let us first analyze the competition between a conventional s-wave harmonic and a monopole superconducting phase. For this purpose, we consider the pairings $\Delta_{\mathbf{k}}^{\text{intra}} = \Delta_s Y_{0,0}(\theta_{\mathbf{k}}, \phi_{\mathbf{k}})$ and $\Delta_{\mathbf{k}}^{\text{inter}} = \bar{\Delta}_{\nu} \mathcal{Y}_{-\nu,\nu,0}(\theta_{\mathbf{k}}, \phi_{\mathbf{k}})$, corresponding to $f_{\text{intra}}(\theta) \sim 1$ and $f_{\text{inter}}(\theta) \sim \sin^{\nu} \theta$, respectively. Therefore, we are in Case 2, and hence applying Eq. (45) we have

$$\begin{aligned} \frac{1}{\lambda_{\eta}} &= \frac{1}{B_{\nu}} \int_0^1 \frac{dxx}{\sqrt{1-x^{2\nu}}} |f_{\eta}(\theta_x)|^2 \left\{ 2 \ln(2\omega_D) \right. \\ &\left. - \ln \left[\frac{1}{2} (\Delta_s^2 + \bar{\Delta}_{\nu}^2 \sin^{2\nu} \theta_x + |\Delta_s^2 - \bar{\Delta}_{\nu}^2 \sin^{2\nu} \theta_x|) \right] \right\}. \end{aligned} \quad (47)$$

We first analyze the situation $\Delta_s \gg \bar{\Delta}_{\nu}$, for which we obtain the following

$$\begin{aligned} \frac{1}{\lambda_{\text{intra}}} &= \frac{1}{B_{\nu}} \int_0^1 \frac{dxx}{\sqrt{1-x^{2\nu}}} [2 \ln(2\omega_D) - \ln(\Delta_s^2)] \\ &= 2 \ln(2\omega_D) - \ln(\Delta_s^2), \end{aligned} \quad (48)$$

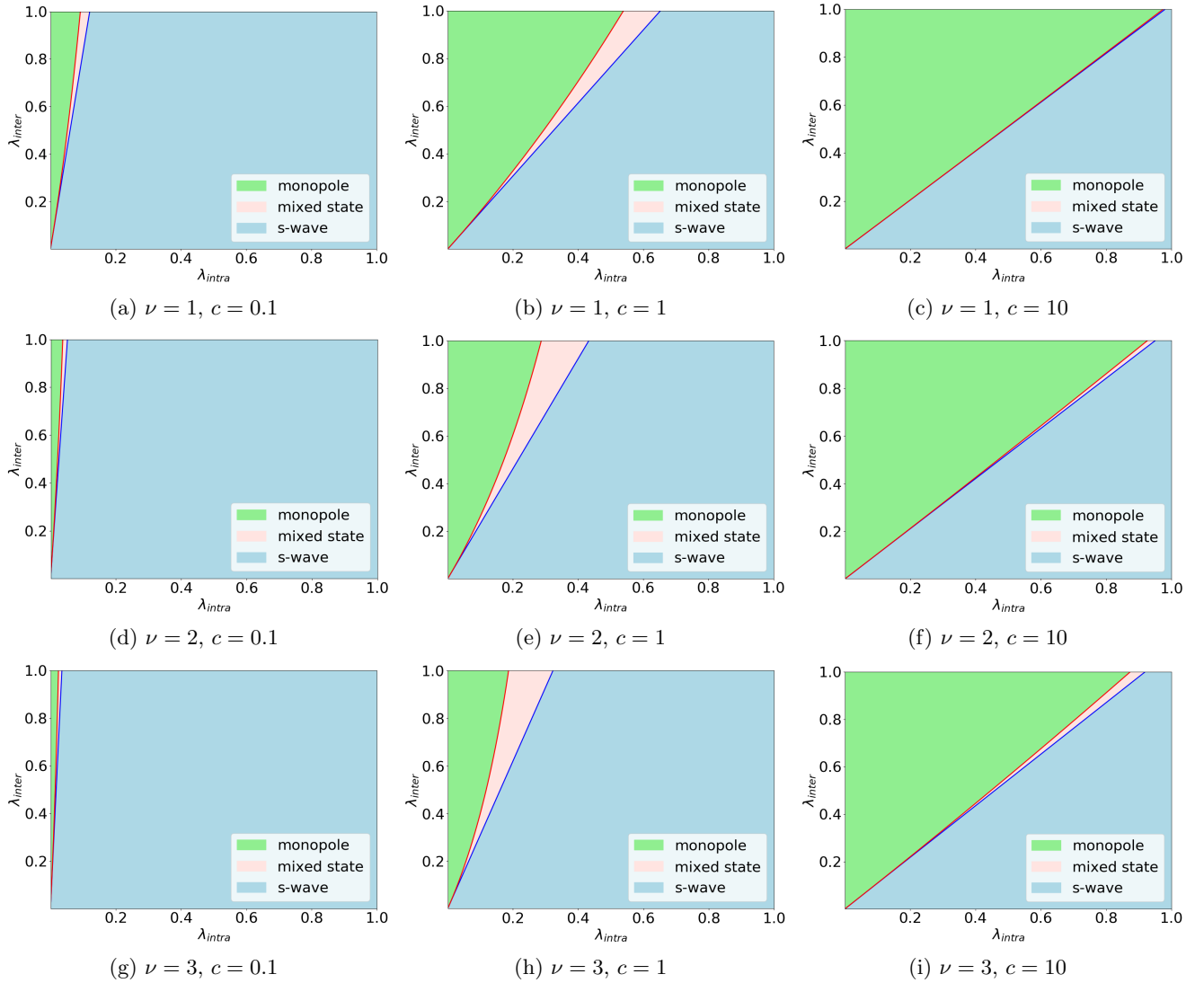


FIG. 1: Phase diagram in the coupling space for **s-wave vs monopole**, for chiralities $\nu = 1, 2, 3$ and $c = 0.1, 1, 10$ to illustrate the behavior when $c \rightarrow 0$, intermediate c and $c \rightarrow \infty$, respectively. Blue line is Eq. (51) and red line is Eq. (58), respectively.

and

$$\begin{aligned} \frac{1}{\lambda_{\text{inter}}} &= \frac{1}{B_\nu} \int_0^1 \frac{dx x}{\sqrt{1-x^{2\nu}}} \sin^{2\nu} \theta_x [2 \ln(2\omega_D) - \ln(\Delta_s^2)] \\ &= I_\nu(c) [2 \ln(2\omega_D) - \ln(\Delta_s^2)], \end{aligned} \quad (49)$$

where we defined the coefficient;

$$I_\nu(c) = \frac{1}{B_\nu} \int_0^1 \frac{dx x}{\sqrt{1-x^{2\nu}}} \sin^{2\nu} \theta_x, \quad (50)$$

for θ_x defined in Eq. (38). Combining Eqs. (48) and (49), we obtain

$$\frac{1}{\lambda_{\text{inter}}} = I_\nu(c) \frac{1}{\lambda_{\text{intra}}}. \quad (51)$$

This equation defines the boundary across which the s-wave dominates over the monopole in the phase diagram.

For the case $\Delta_s \ll \bar{\Delta}_\nu$, we define θ' so that $\sin^\nu \theta' = \Delta_s / \bar{\Delta}_\nu$, with $\theta' \rightarrow 0$. We also define x' according to $\theta_{x=x'} = \theta'$, so that $x' \rightarrow 0$. With these definitions, Eq. (45) reduces to the expression

$$\begin{aligned} \frac{1}{\lambda_\eta} &= \frac{1}{B_\nu} \int_0^1 \frac{dx x |f_\eta(\theta_x)|^2}{\sqrt{1-x^{2\nu}}} \left\{ 2 \ln(2\omega_D) \right. \\ &\quad \left. - \ln \left[\frac{\Delta_s^2}{2} \left(1 + \frac{\sin^{2\nu} \theta_x}{\sin^{2\nu} \theta'} + \left| 1 - \frac{\sin^{2\nu} \theta_x}{\sin^{2\nu} \theta'} \right| \right) \right] \right\}. \end{aligned} \quad (52)$$

To compute the integral in x , we split the domain into

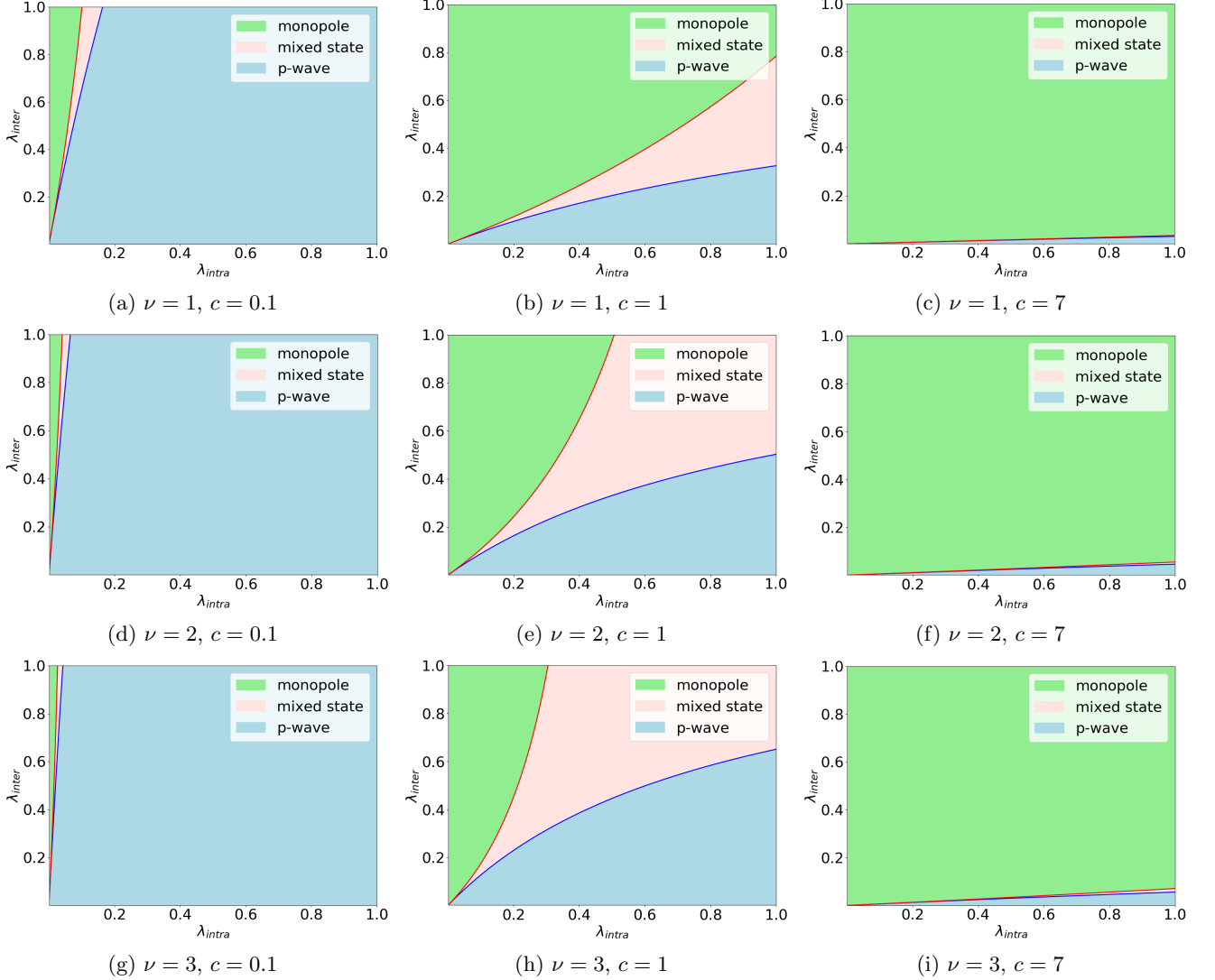


FIG. 2: Phase diagram in the coupling space for **p_z -wave vs monopole**, for chiralities $\nu = 1, 2, 3$ and $c = 0.1, 1, 7$ to illustrate the behavior when $c \rightarrow 0$, intermediate c and $c \rightarrow \infty$, respectively. Blue line is Eq. (62) and red line is Eq. (66), respectively.

intervals $x \in [0, x'] \cup [x', 1]$. Therefore, we have

$$\begin{aligned} \frac{1}{\lambda_\eta} = & \frac{1}{B_\nu} \int_0^1 \frac{dx x |f_\eta(\theta_x)|^2}{\sqrt{1-x^{2\nu}}} [2 \ln(2\omega_D) - \ln(\Delta_s^2)] \\ & + \frac{1}{B_\nu} \int_{x'}^1 \frac{dx x |f_\eta(\theta_x)|^2}{\sqrt{1-x^{2\nu}}} \ln(\sin^{2\nu} \theta') \\ & - \frac{1}{B_\nu} \int_{x'}^1 \frac{dx x |f_\eta(\theta_x)|^2}{\sqrt{1-x^{2\nu}}} \ln(\sin^{2\nu} \theta_x). \end{aligned} \quad (53)$$

Furthermore, we introduce the additional splitting $\int_{x'}^1 = \int_0^1 - \int_0^{x'}$ only in the last integral. Since $x' \rightarrow 0$, the integral $\int_0^{x'}$ can be accurately calculated with the mean value theorem, substituting the factor $\ln(\sin^{2\nu} \theta_x) \approx \ln(\sin^{2\nu} \theta')$ to join it with the second integral in (53).

Thus, after this procedure, we obtain

$$\begin{aligned} \frac{1}{\lambda_\eta} = & \frac{1}{B_\nu} \int_0^1 \frac{dx x |f_\eta(\theta_x)|^2}{\sqrt{1-x^{2\nu}}} \left[2 \ln(2\omega_D) + \ln\left(\frac{\sin^{2\nu} \theta'}{\Delta_s^2}\right) \right] \\ & - \frac{1}{B_\nu} \int_0^1 \frac{dx x |f_\eta(\theta_x)|^2}{\sqrt{1-x^{2\nu}}} \ln(\sin^{2\nu} \theta_x). \end{aligned} \quad (54)$$

Expressing this equation for $\eta = \text{inter}$ and $\eta = \text{intra}$, respectively, we obtain

$$\begin{aligned} \frac{1}{\lambda_{\text{intra}}} = & 2 \ln(2\omega_D) + \ln\left(\frac{\sin^{2\nu} \theta'}{\Delta_s^2}\right) + I_{s\nu}(c) \quad (55) \\ \frac{1}{\lambda_{\text{inter}}} = & I_\nu(c) \left[2 \ln(2\omega_D) + \ln\left(\frac{\sin^{2\nu} \theta'}{\Delta_s^2}\right) \right] + I_{\nu\nu}(c), \end{aligned}$$

where we defined

$$I_{s\nu}(c) = -\frac{1}{B_\nu} \int_0^1 \frac{dxx}{\sqrt{1-x^{2\nu}}} \ln(\sin^{2\nu} \theta_x) \quad (56)$$

$$I_{\nu\nu}(c) = -\frac{1}{B_\nu} \int_0^1 \frac{dxx \sin^{2\nu} \theta_x}{\sqrt{1-x^{2\nu}}} \ln(\sin^{2\nu} \theta_x). \quad (57)$$

Combining both equations, we finally obtain the following result

$$\frac{1}{\lambda_{\text{inter}}} = I_\nu(c) \left[\frac{1}{\lambda_{\text{intra}}} - I_{s\nu}(c) \right] + I_{\nu\nu}(c). \quad (58)$$

This equation determines the boundary across which the monopole predominates over the s-wave.

From (51) and (58), we can construct the phase diagram λ_{inter} versus λ_{intra} for any value of ν and c . Some explicit examples are shown in Fig. 1.

C. p-wave vs Monopole

Similarly to the previous case, we shall now study the coexistence of a conventional spherical harmonic p_z wave with the superconducting monopole. Therefore, we assume for the pairings $\Delta_{\mathbf{k}}^{\text{intra}} = \Delta_{p_z} Y_{1,0}(\theta_{\mathbf{k}}, \phi_{\mathbf{k}})$ and $\Delta_{\mathbf{k}}^{\text{inter}} = \bar{\Delta}_\nu \mathcal{Y}_{-\nu,0}(\theta_{\mathbf{k}}, \phi_{\mathbf{k}})$, with which $f_{\text{intra}}(\theta) \sim \cos \theta$ and $f_{\text{inter}}(\theta) \sim \sin^\nu \theta$, respectively.

Defining θ' so that $\Delta_{p_z}^2 / \bar{\Delta}_\nu^2 = \sin^{2\nu} \theta' / \cos^2 \theta'$, we have after Eq. (45)

$$\frac{1}{\lambda_\eta} = \frac{1}{B_\nu} \int_0^1 \frac{dxx |f_\eta(\theta_x)|^2}{\sqrt{1-x^{2\nu}}} \left\{ 2 \ln(2\omega_D) - \ln \left[\frac{\Delta_{p_z}^2 \cos^2 \theta_x}{2} (1 + g(\theta_x) + |1 - g(\theta_x)|) \right] \right\}, \quad (59)$$

where we defined the function

$$g(\theta_x) = \left(\frac{\sin^{2\nu} \theta_x}{\cos^2 \theta_x} \right) \left(\frac{\cos^2 \theta'}{\sin^{2\nu} \theta'} \right). \quad (60)$$

In addition, we define x' such that $\theta_{x=x'} \equiv \theta'$. By splitting the integration region into subintervals $x \in [0, x'] \cup [x', 1]$, we obtain

$$\frac{1}{\lambda_\eta} = \frac{1}{B_\nu} \int_0^1 \frac{dxx |f_\eta(\theta_x)|^2}{\sqrt{1-x^{2\nu}}} [2 \ln(2\omega_D) - \ln(\Delta_{p_z}^2 \cos^2 \theta_x)] - \frac{1}{B_\nu} \int_{x'}^1 \frac{dxx |f_\eta(\theta_x)|^2}{\sqrt{1-x^{2\nu}}} \ln[g(\theta_x)]. \quad (61)$$

For $\Delta_{p_z} \gg \bar{\Delta}_\nu$, $x' \rightarrow 1$, the last integral vanishes and we obtain

$$\frac{1}{\lambda_{\text{inter}}} = \frac{I_\nu(c)}{I_p(c)} \left[\frac{1}{\lambda_{\text{intra}}} - I_{pp}(c) \right] + I_{\nu p}(c) \quad (62)$$

with

$$I_p(c) = \frac{1}{B_\nu} \int_0^1 \frac{dxx}{\sqrt{1-x^{2\nu}}} \cos^2 \theta_x \quad (63)$$

$$I_{pp}(c) = -\frac{1}{B_\nu} \int_0^1 \frac{dxx}{\sqrt{1-x^{2\nu}}} \cos^2 \theta_x \ln(\cos^2 \theta_x) \quad (64)$$

$$I_{\nu p}(c) = -\frac{1}{B_\nu} \int_0^1 \frac{dxx}{\sqrt{1-x^{2\nu}}} \sin^{2\nu} \theta_x \ln(\cos^2 \theta_x) \quad (65)$$

The case $\Delta_{p_z} \ll \bar{\Delta}_\nu$ is analogous to that of the s wave, thus reducing to the expression

$$\frac{1}{\lambda_{\text{inter}}} = \frac{I_\nu(c)}{I_p(c)} \left[\frac{1}{\lambda_{\text{intra}}} - I_{p\nu}(c) \right] + I_{\nu\nu}(c), \quad (66)$$

along with the definition

$$I_{p\nu}(c) = -\frac{1}{B_\nu} \int_0^1 \frac{dxx}{\sqrt{1-x^{2\nu}}} \cos^2 \theta_x \ln(\sin^{2\nu} \theta_x). \quad (67)$$

In Figure 2 we show the p_z -wave vs monopole phase diagram for different values of ν and c .

V. CRITICAL BEHAVIOR

In this section, we shall analyze the critical temperatures and the corresponding critical exponents that determine the two superconducting phases, i.e. conventional and monopole. Proceeding along the same simplification steps presented in Section IV, we can write the system of BCS Equations (33) at finite temperature in the form

$$\frac{\Delta_\eta}{\lambda_\eta} = C_\eta \Delta_\eta + D_\eta \Delta_{\bar{\eta}} \quad (68)$$

where for notational convenience we use the indexes $\eta = 0 \equiv \text{"intra"}$, $\eta = 1 \equiv \text{"inter"}$, and we define $\bar{\eta} = 1 - \eta$. Consequently, we shall index the order parameters as $\Delta_{l,m'} \equiv \Delta_0$ and $\bar{\Delta}_\nu \equiv \Delta_1$, respectively. In this more convenient and compact notation, we define the coefficients

$$C_\eta(\Delta_0, \Delta_1) = \frac{1}{B_\nu} \int_0^1 \frac{xf_\eta^2(\theta_x)dx}{\sqrt{1-x^{2\nu}}} \int_0^{2\pi} \frac{d\phi}{2\pi} \times \int_0^{\omega_D} d\xi [\mathcal{T}_\beta(\Gamma) + \mathcal{T}_\beta(\gamma)], \quad (69)$$

along with the function

$$\mathcal{T}_\beta(z) \equiv \frac{\tanh(\beta z/2)}{z}. \quad (70)$$

Similarly, for $r \equiv m' - m - \nu$, we define the coefficients

$$D_\eta(\Delta_0, \Delta_1) = \frac{1}{B_\nu} \int_0^1 \frac{xf_\eta(\theta_x)f_{\bar{\eta}}(\theta_x)dx}{\sqrt{1-x^{2\nu}}} \int_0^{2\pi} \frac{d\phi}{2\pi} e^{\pm ir\phi} \times \int_0^{\omega_D} d\xi [\mathcal{T}_\beta(\Gamma) - \mathcal{T}_\beta(\gamma)]. \quad (71)$$

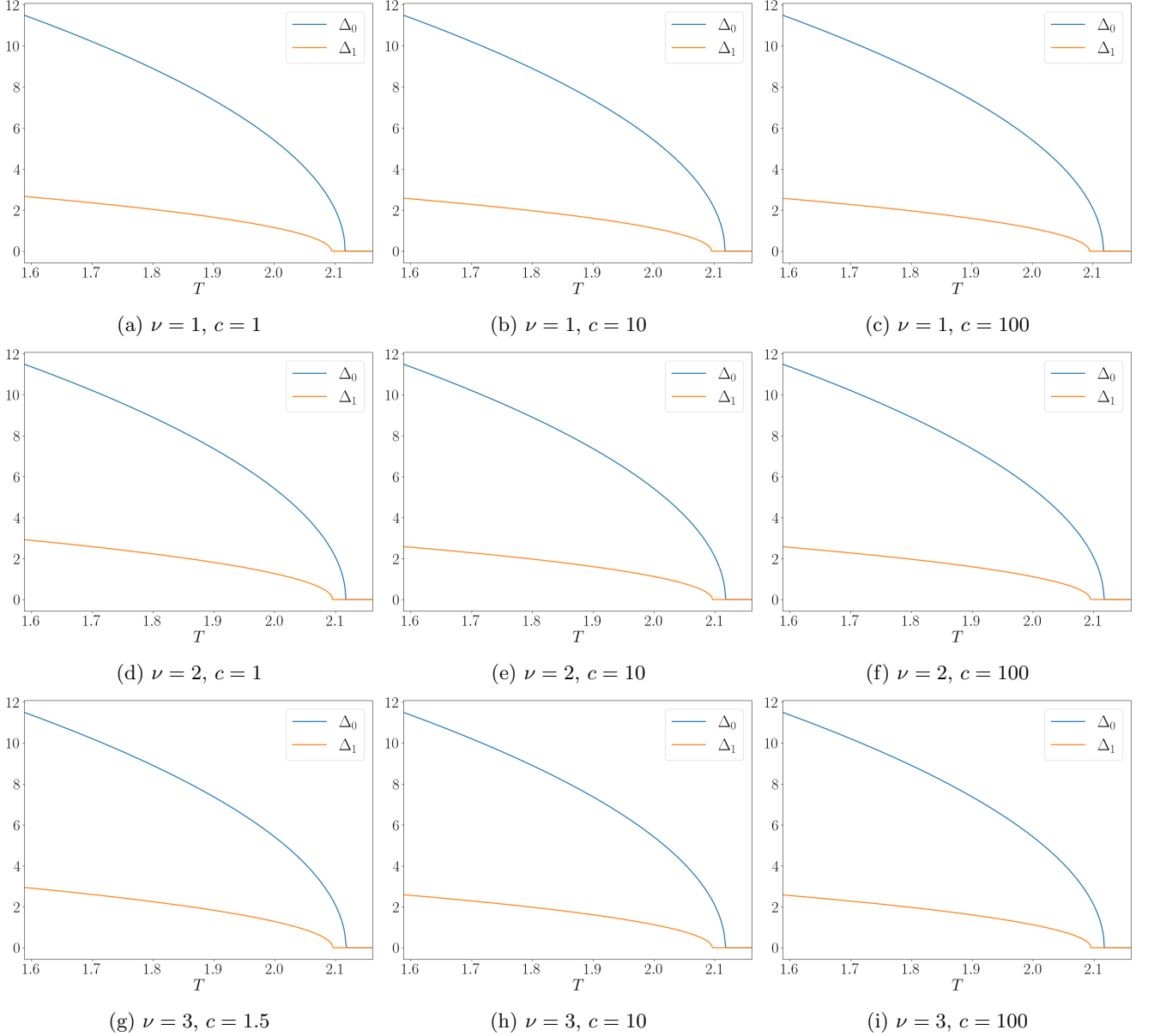


FIG. 3: Pairings Δ_0 (s-wave in the intra-nodal channel) and Δ_1 (monopole in the inter-nodal channel), both in units of $10^{-3}\hbar\omega_D$, as function of T (in units of $10^{-3}\hbar\omega_D/k_B$) near the critical temperatures.

where we defined the functions (ignoring any asymmetry in the chemical potential $\delta\mu = 0$)

$$\begin{aligned} \Gamma &= [\xi^2 + \Delta_0^2 f_{intra}^2(\theta_x) + \Delta_1^2 f_{inter}^2(\theta_x) \\ &\quad + 2\Delta_0\Delta_1 f_{intra}(\theta_x)f_{inter}(\theta_x)\cos(r\phi)]^{1/2} \\ \gamma &= [\xi^2 + \Delta_0^2 f_{intra}^2(\theta_x) + \Delta_1^2 f_{inter}^2(\theta_x) \\ &\quad - 2\Delta_0\Delta_1 f_{intra}(\theta_x)f_{inter}(\theta_x)\cos(r\phi)]^{1/2} \end{aligned} \quad (72)$$

Let us start by considering two critical temperatures T_0^c , T_1^c , each of them associated to the vanishing conditions of the corresponding order parameter: $\Delta_\eta(T \rightarrow T_\eta^c) = 0$ for $\eta = 0, 1$ (intra/inter).

Without loss of generality, from now on we choose the

index η such that it corresponds to the highest critical temperature, i.e.

$$T_\eta^c = \text{Max} \{T_0^c, T_1^c\}, \quad (73)$$

and hence $T_\eta^c > T_{\bar{\eta}}^c$, for $\bar{\eta} = 1 - \eta$. Under this prescription, let us first consider the region $T \lesssim T_\eta^c$. Then, while $\Delta_{\bar{\eta}} \equiv 0$ in this temperature zone, we may cancel the factor Δ_η on both sides, and afterward take the limit

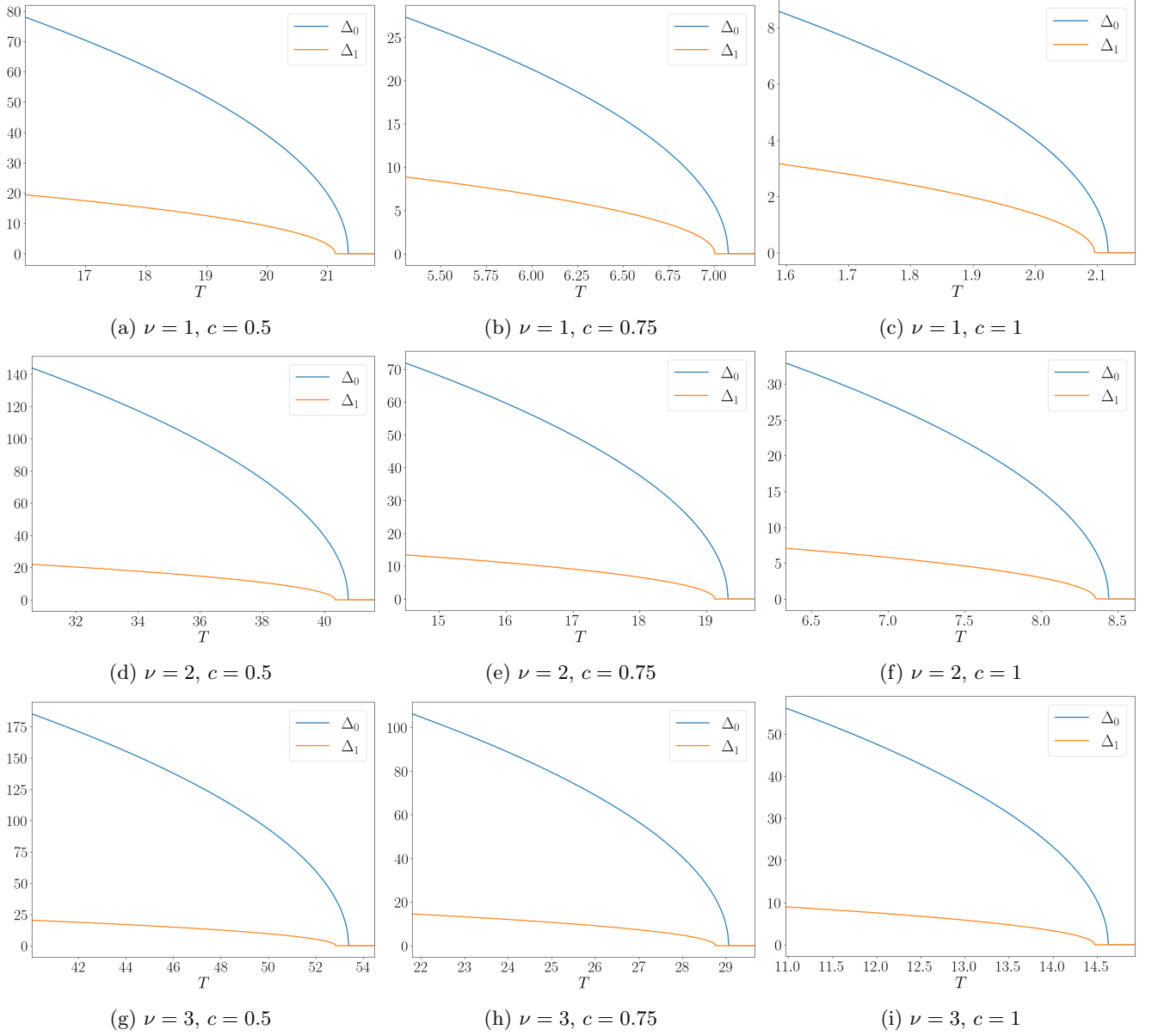


FIG. 4: Pairings Δ_0 (p_z -wave in the intra-nodal channel) and Δ_1 (monopole in the inter-nodal channel), both in

units of $10^{-3}\hbar\omega_D$

, as function of T (in units of $10^{-3}\hbar\omega_D/k_B$) near the critical temperatures.

$\lim_{T \rightarrow T_\eta^{c-}} \Delta_\eta(T) = 0$ in Eq. (68), to obtain

$$\begin{aligned} \frac{1}{\lambda_\eta} &= \lim_{\Delta_\eta \rightarrow 0} C_\eta(\Delta_\eta, \Delta_{\bar{\eta}} = 0) = \Lambda_{\eta\bar{\eta}}^{20} \int_0^{\frac{\omega_D}{2T_\eta^c}} dz \frac{\tanh(z)}{z} \\ &\simeq \Lambda_{\eta\bar{\eta}}^{20} \ln \left(\frac{2}{\pi} e^{\gamma_E} \frac{\omega_D}{T_\eta^c} \right), \end{aligned} \quad (74)$$

where γ_E is the Euler-Mascheroni constant, and we defined the angular integrals

$$\Lambda_{\eta\bar{\eta}}^{nm} \equiv \frac{2}{B_\nu} \int_0^1 \frac{dx}{\sqrt{1-x^{2\nu}}} f_\eta^n(\theta_x) f_{\bar{\eta}}^m(\theta_x). \quad (75)$$

Solving explicitly from Eq. (74), we obtain the highest critical temperature as

$$T_\eta^c = \frac{2\omega_D}{\pi} e^{\gamma_E} e^{-\frac{1}{\lambda_\eta \Lambda_{\eta\bar{\eta}}^{20}}}. \quad (76)$$

Based on this first result, we then conclude that the highest critical temperature T_η^c will depend, in terms of the microscopic parameters of the model, upon the condition $\text{Max}\{\lambda_1 \Lambda_{10}^{20}, \lambda_0 \Lambda_{10}^{02}\}$.

Let us now consider the interval between the two critical temperatures, i.e. $T_\eta^c < T < T_{\bar{\eta}}^c$. Therefore, the condition $\Delta_{\bar{\eta}}(T) \equiv 0$ still applies, but $\Delta_\eta(T) \neq 0$. We can thus expand the functions in the integrand of Eq. (69)

up to second-order in $\Delta_\eta(T)$, as follows

$$\frac{\mathcal{T}_\beta(\Gamma) + \mathcal{T}_\beta(\gamma)}{2} \simeq \frac{\tanh\left(\frac{\beta\xi}{2}\right)}{\xi} + \frac{\Delta_\eta^2 f_\eta^2(\theta_x)}{16} \psi_\beta\left(\frac{\beta\xi}{2}\right), \quad (77)$$

where we defined the function

$$\psi_\beta(z) = \frac{\beta^3}{z^3} [z \operatorname{sech}^2(z) - \tanh(z)]. \quad (78)$$

Substituting these relations into Eq. (68), we obtain (for $T_{\bar{\eta}}^c < T < T_\eta^c$)

$$\begin{aligned} \frac{1}{\lambda_\eta} &= C_\eta(\Delta_\eta, \Delta_{\bar{\eta}} = 0) \\ &= \Lambda_{\eta\bar{\eta}}^{20} \ln\left(\frac{2}{\pi} e^{\gamma_E} \frac{\omega_D}{T}\right) - \alpha \Lambda_{\eta\bar{\eta}}^{40} \frac{\Delta_\eta^2(T)}{T^2}, \end{aligned} \quad (79)$$

with $\alpha = 7\zeta(3)/(8\pi^2) \sim 0.10657$ and $\zeta(3) \sim 1.202$ the Riemann zeta function. Substituting the definition of the highest critical temperature from Eq. (74) into Eq. (79), we obtain the temperature dependence of the corresponding order parameter

$$\Delta_\eta^2(T) = \frac{\Lambda_{\eta\bar{\eta}}^{20}}{\Lambda_{\eta\bar{\eta}}^{40}} \frac{T^2}{\alpha} \ln\left(\frac{T_\eta^c}{T}\right) \sim \kappa_\eta |T_\eta^c - T|, \quad (80)$$

with $\kappa_\eta = \frac{\Lambda_{\eta\bar{\eta}}^{20}}{\Lambda_{\eta\bar{\eta}}^{40}} \frac{T_\eta^c}{\alpha}$. This clearly shows that the corresponding critical exponent is $1/2$, just as in the standard BCS theory.

In order to investigate the lowest critical temperature $T_{\bar{\eta}}^c$, let us now consider the second equation in the system Eq. (68) corresponding to $\bar{\eta}$, and take the limit $T \rightarrow T_{\bar{\eta}}^{c-}$, where $\Delta_{\bar{\eta}} \rightarrow 0$, but $\Delta_\eta \neq 0$,

$$\frac{1}{\lambda_{\bar{\eta}}} = C_{\bar{\eta}}(\Delta_\eta, \Delta_{\bar{\eta}} = 0) + \lim_{\Delta_{\bar{\eta}} \rightarrow 0} D_{\bar{\eta}}(\Delta_\eta, \Delta_{\bar{\eta}}) \cdot \frac{\Delta_\eta}{\Delta_{\bar{\eta}}} \quad (81)$$

The limit in the second term above is obtained by first using the expansion

$$\mathcal{T}_\beta(\Gamma) - \mathcal{T}_\beta(\gamma) \simeq \frac{\Delta_\eta \Delta_{\bar{\eta}}}{4} f_\eta(\theta_x) f_{\bar{\eta}}(\theta_x) \cos(r\phi) \psi_\beta\left(\frac{\beta\xi}{2}\right) \quad (82)$$

in Eq. (71), and by further applying the identity

$$\int_0^{2\pi} \frac{d\phi}{2\pi} e^{\pm ir\phi} \cos(r\phi) = \frac{1 + \delta_{r,0}}{2}. \quad (83)$$

Therefore, we obtain

$$\lim_{\Delta_{\bar{\eta}} \rightarrow 0} D_{\bar{\eta}}(\Delta_\eta, \Delta_{\bar{\eta}}) \cdot \frac{\Delta_\eta}{\Delta_{\bar{\eta}}} = -\alpha(1 + \delta_{r,0}) \Lambda_{\eta\bar{\eta}}^{22} \frac{\Delta_\eta^2(T_{\bar{\eta}}^c)}{T_{\bar{\eta}}^{c2}}. \quad (84)$$

Substituting this result into Eq. (81), and assuming that the two critical temperatures are close enough so we can still use Eq. (80) for $\Delta_\eta(T)$, we obtain the expression

$$\frac{1}{\Lambda_{\eta\bar{\eta}}^{02} \lambda_{\bar{\eta}}} = \ln\left(\frac{2}{\pi} e^{\gamma_E} \frac{\omega_D}{T_{\bar{\eta}}^c}\right) - (2 + \delta_{r,0}) \frac{\Lambda_{\eta\bar{\eta}}^{22} \Lambda_{\eta\bar{\eta}}^{20}}{\Lambda_{\eta\bar{\eta}}^{02} \Lambda_{\eta\bar{\eta}}^{40}} \ln\left(\frac{T_\eta^c}{T_{\bar{\eta}}^c}\right) \quad (85)$$

Subtracting Eq. (74) from Eq. (85), after some elementary algebra we obtain

$$\frac{1}{\lambda_{\bar{\eta}} \Lambda_{\eta\bar{\eta}}^{02}} - \frac{1}{\lambda_\eta \Lambda_{\eta\bar{\eta}}^{20}} = \frac{1}{\sigma_r} \ln\left(\frac{T_\eta^c}{T_{\bar{\eta}}^c}\right), \quad (86)$$

where we defined the parameter

$$1/\sigma_r = 1 - (2 + \delta_{r,0}) \frac{\Lambda_{\eta\bar{\eta}}^{20} \Lambda_{\eta\bar{\eta}}^{22}}{\Lambda_{\eta\bar{\eta}}^{02} \Lambda_{\eta\bar{\eta}}^{40}}. \quad (87)$$

From Eq. (86), we obtain the expression

$$T_{\bar{\eta}}^c = T_\eta^c e^{-\sigma_r \left(\frac{1}{\lambda_{\bar{\eta}} \Lambda_{\eta\bar{\eta}}^{02}} - \frac{1}{\lambda_\eta \Lambda_{\eta\bar{\eta}}^{20}} \right)}. \quad (88)$$

This result implies a necessary condition for the existence of the lowest temperature superconducting phase $\Delta_{\bar{\eta}}(T) \neq 0$, i.e. that $\sigma_r \left(\frac{1}{\lambda_{\bar{\eta}} \Lambda_{\eta\bar{\eta}}^{02}} - \frac{1}{\lambda_\eta \Lambda_{\eta\bar{\eta}}^{20}} \right) > 0$.

Finally, in the low temperature region $T < T_{\bar{\eta}}^c$, both order parameters acquire small finite values, such that applying a similar expansion procedure as described before, we find that the coefficients in the system Eq. (68) are given (up to second order) by

$$\begin{aligned} C_\eta &\simeq \Lambda_{\eta\bar{\eta}}^{20} \ln\left(\frac{2}{\pi} e^{\gamma_E} \frac{\omega_D}{T}\right) - \frac{\alpha}{T^2} (\Lambda_{\eta\bar{\eta}}^{40} \Delta_\eta^2 + \Lambda_{\eta\bar{\eta}}^{22} \Delta_{\bar{\eta}}^2) \\ C_{\bar{\eta}} &\simeq \Lambda_{\eta\bar{\eta}}^{02} \ln\left(\frac{2}{\pi} e^{\gamma_E} \frac{\omega_D}{T}\right) - \frac{\alpha}{T^2} (\Lambda_{\eta\bar{\eta}}^{04} \Delta_{\bar{\eta}}^2 + \Lambda_{\eta\bar{\eta}}^{22} \Delta_\eta^2) \\ D_\eta = D_{\bar{\eta}} &\simeq -\frac{\alpha(1 + \delta_{r,0})}{T^2} \Lambda_{\eta\bar{\eta}}^{22} \Delta_\eta \Delta_{\bar{\eta}} \end{aligned} \quad (89)$$

Inserting these expressions into the system Eq. (68), canceling common factors, and substituting the coupling constants in terms of both critical temperatures, we end up with the linear system

$$\frac{\Lambda_{\eta\bar{\eta}}^{40}}{\Lambda_{\eta\bar{\eta}}^{20}} \Delta_\eta^2 + \frac{\Lambda_{\eta\bar{\eta}}^{22}}{\Lambda_{\eta\bar{\eta}}^{20}} (2 + \delta_{r,0}) \Delta_{\bar{\eta}}^2 = -\frac{T^2}{\alpha} \ln\left(\frac{T}{T_\eta^c}\right) \quad (90)$$

$$\frac{\Lambda_{\eta\bar{\eta}}^{04}}{\Lambda_{\eta\bar{\eta}}^{02}} \Delta_{\bar{\eta}}^2 + \frac{\Lambda_{\eta\bar{\eta}}^{22}}{\Lambda_{\eta\bar{\eta}}^{02}} (2 + \delta_{r,0}) \Delta_\eta^2 = -\frac{T^2}{\alpha} \ln\left[\left(\frac{T}{T_\eta^c}\right) \left(\frac{T_\eta^c}{T_{\bar{\eta}}^c}\right)^{\frac{1}{\sigma_r}}\right]$$

By explicitly solving this linear system for the order parameters, we finally obtain, in the region close to the lower critical temperature $0 < T \lesssim T_{\bar{\eta}}^c$

$$\begin{aligned} \Delta_\eta^2(T) &= q_r \frac{T^2}{\alpha} \ln\left(\frac{T_\eta^c}{T_{\bar{\eta}}^c}\right) - p_r \frac{T^2}{\alpha} \ln\left(\frac{T}{T_\eta^c}\right) \\ \Delta_{\bar{\eta}}^2(T) &= -\bar{p}_r \frac{T^2}{\alpha} \ln\left(\frac{T}{T_{\bar{\eta}}^c}\right) \simeq \kappa_{\bar{\eta}} |T - T_{\bar{\eta}}^c|. \end{aligned} \quad (91)$$

Here, we define the coefficients

$$\begin{aligned}
q_r &\equiv \frac{\Lambda_{\eta\bar{\eta}}^{22}\Lambda_{\eta\bar{\eta}}^{02}(2 + \delta_{r,0})}{\sigma_r \left[\Lambda_{\eta\bar{\eta}}^{40}\Lambda_{\eta\bar{\eta}}^{04} - (2 + \delta_{r,0})^2 \left(\Lambda_{\eta\bar{\eta}}^{22} \right)^2 \right]} \\
p_r &\equiv \frac{\Lambda_{\eta\bar{\eta}}^{04}\Lambda_{\eta\bar{\eta}}^{20} - (2 + \delta_{r,0})\Lambda_{\eta\bar{\eta}}^{22}\Lambda_{\eta\bar{\eta}}^{02}}{\left[\Lambda_{\eta\bar{\eta}}^{40}\Lambda_{\eta\bar{\eta}}^{04} - (2 + \delta_{r,0})^2 \left(\Lambda_{\eta\bar{\eta}}^{22} \right)^2 \right]} \\
\bar{p}_r &\equiv \frac{\Lambda_{\eta\bar{\eta}}^{40}\Lambda_{\eta\bar{\eta}}^{02} - (2 + \delta_{r,0})\Lambda_{\eta\bar{\eta}}^{22}\Lambda_{\eta\bar{\eta}}^{20}}{\left[\Lambda_{\eta\bar{\eta}}^{40}\Lambda_{\eta\bar{\eta}}^{04} - (2 + \delta_{r,0})^2 \left(\Lambda_{\eta\bar{\eta}}^{22} \right)^2 \right]} \\
\kappa_{\bar{\eta}} &\equiv \frac{\bar{p}_r T_{\eta}^c}{\alpha} \tag{92}
\end{aligned}$$

We present explicit numerical examples of the temperature dependence of both pairings in Fig. 3 for the s-wave and in Fig. 4 for the p-wave, respectively. As can be observed in both figures, the critical behavior of these order parameters is qualitatively similar, as follows from the previous mathematical analysis in the vicinity of the critical temperatures. Clearly, in agreement with Eq. (76), the numerical value of each critical temperature T_0^c and T_1^c is established by the angular dependence of the corresponding order parameters, and by the topological charge ν , via the angular integrals Eq. (75). In particular, for the two examples considered here, i.e., the s-wave in Fig. 3 and the p-wave in Fig. 4, the critical temperature associated with the monopole (inter-nodal) is slightly lower than the corresponding to conventional spherical harmonic (intra-nodal) $T_1^c < T_0^c$, for all three topological charges $\nu = 1, 2, 3$. On the other hand, we see that for the s-wave in Fig. 3, the order parameters become practically independent of the parameter c , for relatively large values $c > 1$. In contrast, for the p-wave in Fig. 4 we see that there is a strong dependence on this parameter in the region $c < 1$.

VI. SPECIFIC HEAT

In cases where both superconducting phases coexist, we expect two superconducting phase transitions to exist at the corresponding critical temperatures, which are likely to be different. As a possible experimental probe for these transitions, we seek to calculate the specific heat of the system as a function of temperature, since we expect a discontinuous jump in the specific heat at each critical point.

For this purpose, we first calculate the internal energy of the system from the grand canonical partition function, according to the general expression

$$\langle \hat{H} \rangle = -\frac{\partial}{\partial \beta} \ln \mathcal{Z} + \frac{\mu}{\beta} \frac{\partial}{\partial \mu} \ln \mathcal{Z}. \tag{93}$$

The contribution to the partition function associated with the superconducting phases is calculated from the

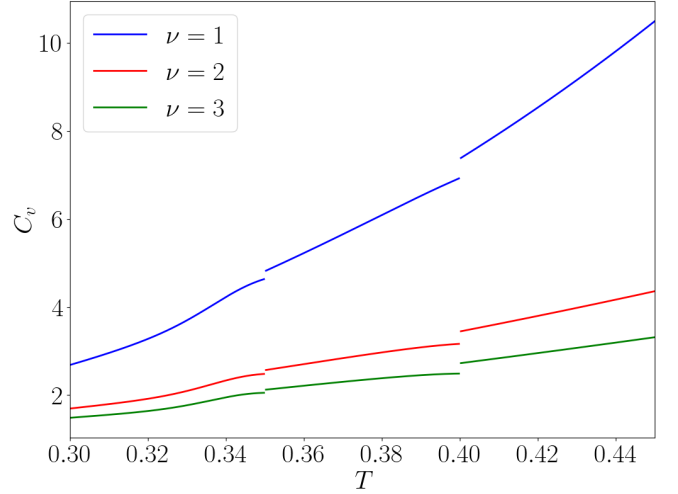


FIG. 5: Total specific heat $C_v = C_v^{\text{norm}} + C_v^{SC}$ (in units of $k_B \omega_D / [v_f \alpha_{\nu}^{2/(\nu-1)}]$), as function of temperature (in units of $\hbar v_f \alpha_{\nu}^{1/(1-\nu)} / k_B$), for $\nu = 1, 2, 3$. Notice that α_{ν} has.

finite-temperature Green's function of our effective model in the Matsubara frequency space.

$$\begin{aligned}
\ln \mathcal{Z}^{SC} &= \ln \left(\det[\hat{\mathcal{G}}_{\mathbf{k}}^{-1}(\omega_n)] \right) = -\text{Tr} \left[\ln \hat{\mathcal{G}}_{\mathbf{k}}(\omega_n) \right] \\
&= \sum_{\mathbf{k}, \omega_n} \ln [(\omega_n^2 + \Gamma_{\mathbf{k}}^2)(\omega_n^2 + \gamma_{\mathbf{k}}^2)] \tag{94} \\
&= \sum_{\mathbf{k}} \ln [(1 + \cosh(\beta \Gamma_{\mathbf{k}}))(1 + \cosh(\beta \gamma_{\mathbf{k}}))].
\end{aligned}$$

Then, the specific heat associated with each of the superconducting transitions is calculated as

$$C_v^{SC} = \beta^2 \frac{\partial^2}{\partial \beta^2} \ln \mathcal{Z}^{SC} - \beta^2 \frac{\partial}{\partial \beta} \left(\frac{\mu}{\beta} \frac{\partial}{\partial \mu} \ln \mathcal{Z}^{SC} \right). \tag{95}$$

Here we must consider the temperature dependence of the gap functions to calculate the derivatives. In agreement with⁴⁰, we have

$$|\Delta^{\eta}| \sim |T - T_c^{\eta}|^{1/2}, \tag{96}$$

for both $\eta = \text{intra/inter}$, $T < T_c^{\eta}$ and for a simple WSM with isotropic dispersion relation. Here we will use the same relation, because the development carried out in⁴⁰ can be generalized to multi-WSM obtaining the same critical exponents.

On the other hand, we calculate the specific heat component due to fermions in the normal WSM phase, with energy dispersion $\xi_{\mathbf{k}} = v_f \sqrt{k_z^2 + \alpha^2 k_{\perp}^{2\nu}}$, as follows

$$C_v^{\text{norm}} = \beta^2 \int \frac{d^3 k}{(2\pi)^3} \frac{(\xi_{\mathbf{k}} - \mu)^2 e^{-\beta(\xi_{\mathbf{k}} - \mu)}}{(1 + e^{-\beta(\xi_{\mathbf{k}} - \mu)})^2}. \tag{97}$$

This integral is solved by means of the change of variables

$$\begin{aligned} k_x &= \left(\frac{r}{\alpha_\nu} \sin \theta \right)^{1/\nu} \cos \phi, \\ k_y &= \left(\frac{r}{\alpha_\nu} \sin \theta \right)^{1/\nu} \sin \phi, \\ k_z &= r \cos \theta, \end{aligned} \quad (98)$$

with which we have $\xi_{\mathbf{k}} = v_f r$ and the Jacobian

$$\left| \frac{\partial(k_x, k_y, k_z)}{\partial(r, \theta, \phi)} \right| = \frac{1}{\nu} \left(\frac{r}{\alpha_\nu} \right)^{2/\nu} \sin^{2/\nu-1} \theta. \quad (99)$$

Then, in the limit $\mu \rightarrow 0$ we obtain

$$C_v^{\text{norm}} = \frac{\beta(\frac{1}{\nu}, \frac{1}{2})}{(2\pi)^2 \nu \alpha_\nu^{2/\nu}} \left(\frac{T}{v_f} \right)^{\frac{2}{\nu}+1} \int_0^\infty dx \frac{x^{2+2/\nu} e^{-x}}{(1+e^{-x})^2}. \quad (100)$$

In Figure 5 we plot the total specific heat $C_v^{\text{norm}} + C_v^{SC}$. As expected, the specific heat displays discontinuities precisely at the critical temperatures corresponding to each monopole and conventional superconducting phases, respectively. In addition, as seen in Fig. 5, the curves display different slopes depending on the chiral index $\nu = 1, 2, 3$, which may offer an experimental probe to characterize these topological materials by measuring their specific heat.

VII. DISCUSSION AND CONCLUSIONS

In this work, we presented a theoretical model to explore the possible emergence and competition of conventional and monopole superconducting phases in multi-WSMs, generalizing the previous analysis presented in^{39,40}. We explicitly showed that the order parameters associated to intra-nodal and inter-

nodal pairing, exhibit conventional spherical harmonics $\Delta_{\mathbf{k}}^{\text{intra}} = \Delta_{l,m'} Y_{l,m'}(\theta_{\mathbf{k}}, \phi_{\mathbf{k}}) = \Delta_{l,m'} f_{\text{intra}}(\theta_{\mathbf{k}}) e^{im' \phi_{\mathbf{k}}}$, and monopole harmonics $\Delta_{\mathbf{k}}^{\text{inter}} = \Delta_\nu \mathcal{Y}_{\nu,j,m}(\theta_{\mathbf{k}}, \phi_{\mathbf{k}}) = \Delta_\nu f_{\text{inter}}(\theta_{\mathbf{k}}) e^{i(m+\nu) \phi_{\mathbf{k}}}$ angular dependencies, respectively. According to our model, we have shown that, depending on the nature of the θ -component of the spherical harmonics of the order parameters defined above, it is possible to observe both a conventional and a monopole superconducting phases, separated by a region of coexistence or mixed state. However, we also showed that if the azimuthal indexes of the conventional (m') and monopole (m) satisfy the relation $m' = m + \nu$, and furthermore the $f_{\text{intra}}(\theta) \simeq f_{\text{inter}}(\theta)$, then topological repulsion takes place and hence the coexistence region between both phases disappears, in agreement with³⁹.

We further computed the specific heat as a function of temperature, and we showed that according to our model this property displays discontinuities at the critical temperatures corresponding to each monopole and conventional superconducting phases, respectively. As discussed in Section III, the critical temperatures for both possible superconducting phases depend explicitly on the topological charge ν , as well as on the microscopic parameter c . Moreover, we also showed that the slope of the specific heat curve as a function of temperature strongly depends on the chirality index $\nu = 1, 2, 3$. Both features suggest that, according to our model, the specific heat offers a possible experimental probe to characterize the topological properties of these quantum materials.

ACKNOWLEDGMENTS

E. Muñoz acknowledges financial support from ANID Fondecyt grant No 1230440. A. Tapia acknowledges financial support from ANID-Subdirección de Capital Humano/Magíster Nacional/2024 - 22240909.

* ejmunozt@uc.cl

¹ Shuichi Murakami, “Phase transition between the quantum spin hall and insulator phases in 3d: emergence of a topological gapless phase,” *New Journal of Physics* **9**, 356 (2007).

² A. A. Burkov and Leon Balents, “Weyl semimetal in a topological insulator multilayer,” *Phys. Rev. Lett.* **107**, 127205 (2011).

³ Xiangang Wan, Ari M. Turner, Ashvin Vishwanath, and Sergey Y. Savrasov, “Topological semimetal and fermi-arc surface states in the electronic structure of pyrochlore iridates,” *Phys. Rev. B* **83**, 205101 (2011).

⁴ A.M. Black-Schaffer T.O. Wehling and A.V. Balatsky, “Dirac materials,” *Advances in Physics* **63**, 1–76 (2014), <https://doi.org/10.1080/00018732.2014.927109>.

⁵ C.-K. Chiu, J. C. Y. Teo, A. P. Schnyder, and S. Ryu, “Classification of topological quantum matter with sym-

metries,” *Rev. Mod. Phys.* **88**, 035005 (2016).

⁶ Barry Bradlyn, Jennifer Cano, Zhijun Wang, M. G. Vergniory, C. Felser, R. J. Cava, and B. Andrei Bernevig, “Beyond dirac and weyl fermions: Unconventional quasiparticles in conventional crystals,” *Science* **353**, aaf5037 (2016), <https://www.science.org/doi/pdf/10.1126/science.aaf5037>.

⁷ N. P. Armitage, E. J. Mele, and Ashvin Vishwanath, “Weyl and dirac semimetals in three-dimensional solids,” *Rev. Mod. Phys.* **90**, 015001 (2018).

⁸ A.A. Burkov, “Weyl metals,” *Annual Review of Condensed Matter Physics* **9**, 359–378 (2018).

⁹ Su-Yang Xu, Ilya Belopolski, Nasser Alidoust, Madhab Neupane, Guang Bian, Chenglong Zhang, Raman Sankar, Guoqing Chang, Zhujun Yuan, Chi-Cheng Lee, Shin-Ming Huang, Hao Zheng, Jie Ma, Daniel S. Sanchez, BaoKai Wang, Arun Bansil, Fangcheng Chou,

Pavel P. Shibayev, Hsin Lin, Shuang Jia, and M. Zahid Hasan, "Discovery of a weyl fermion semimetal and topological fermi arcs," *Science* **349**, 613–617 (2015), <https://www.science.org/doi/pdf/10.1126/science.aaa9297>.

¹⁰ Davide Grassano, Olivia Pulci, Adriano Mosca Conte, and Friedhelm Bechstedt, "Validity of weyl fermion picture for transition metals monopnictides taas, tap, nbas, and nbp from ab initio studies," *Scientific Reports* **8**, 3534 (2018).

¹¹ Cheng-Long Zhang, Su-Yang Xu, Ilya Belopolski, Zhujun Yuan, Ziquan Lin, Bingbing Tong, Guang Bian, Nasser Alidoust, Chi-Cheng Lee, Shin-Ming Huang, Tay-Rong Chang, Guoqing Chang, Chuang-Han Hsu, Horng-Tay Jeng, Madhab Neupane, Daniel S. Sanchez, Hao Zheng, Junfeng Wang, Hsin Lin, Chi Zhang, Hai-Zhou Lu, Shun-Qing Shen, Titus Neupert, M. Zahid Hasan, and Shuang Jia, "Signatures of the adler–bell–jackiw chiral anomaly in a weyl fermion semimetal," *Nature Communications* **7**, 10735 (2016).

¹² Frank Arnold, Chandra Shekhar, Shu-Chun Wu, Yan Sun, Ricardo Donizeth dos Reis, Nitesh Kumar, Marcel Naumann, Mukkattu O. Ajeesh, Marcus Schmidt, Adolfo G. Grushin, Jens H. Bardarson, Michael Baenitz, Dmitry Sokolov, Horst Borrman, Michael Nicklas, Claudia Felser, Elena Hassinger, and Binghai Yan, "Negative magnetoresistance without well-defined chirality in the weyl semimetal tap," *Nature Communications* **7**, 11615 (2016).

¹³ Chandra Shekhar, Ajaya K. Nayak, Yan Sun, Marcus Schmidt, Michael Nicklas, Inge Leermakers, Uli Zeitler, Yurii Skourski, Jochen Wosnitza, Zhongkai Liu, Yulin Chen, Walter Schnelle, Horst Borrman, Yuri Grin, Claudia Felser, and Binghai Yan, "Extremely large magnetoresistance and ultrahigh mobility in the topological weyl semimetal candidate nbp," *Nature Physics* **11**, 645–649 (2015).

¹⁴ B. Q. Lv, H. M. Weng, B. B. Fu, X. P. Wang, H. Miao, J. Ma, P. Richard, X. C. Huang, L. X. Zhao, G. F. Chen, Z. Fang, X. Dai, T. Qian, and H. Ding, "Experimental discovery of weyl semimetal taas," *Phys. Rev. X* **5**, 031013 (2015).

¹⁵ Su-Yang Xu, Ilya Belopolski, Nasser Alidoust, Madhab Neupane, Guang Bian, Chenglong Zhang, Raman Sankar, Guoqing Chang, Zhujun Yuan, Chi-Cheng Lee, Shin-Ming Huang, Hao Zheng, Jie Ma, Daniel S. Sanchez, BaoKai Wang, Arun Bansil, Fangcheng Chou, Pavel P. Shibayev, Hsin Lin, Shuang Jia, and M. Zahid Hasan, "Discovery of a weyl fermion semimetal and topological fermi arcs," *Science* **349**, 613–617 (2015).

¹⁶ Cheng-Long Zhang, Zhujun Yuan, Qing-Dong Jiang, Bingbing Tong, Chi Zhang, X. C. Xie, and Shuang Jia, "Electron scattering in tantalum monoarsenide," *Phys. Rev. B* **95**, 085202 (2017).

¹⁷ Su-Yang Xu, Ilya Belopolski, Daniel Sanchez, Chenglong Zhang, Guoqing Chang, Cheng Guo, Guang Bian, Zhujun Yuan, Hong Lu, Tay-Rong Chang, Pavel Shibayev, Mykhailo Prokopovych, Nasser Alidoust, Hao Zheng, Chi-Cheng Lee, Shin-Ming Huang, Raman Sankar, F. Chou, Chuang-Han Hsu, and M. Zahid Hasan, "Experimental discovery of a topological weyl semimetal state in tap," *Science Advances* **1**, e1501092–e1501092 (2015).

¹⁸ N. Xu, Hongming Weng, B. Lv, Christian Matt, J. Park, Federico Bisti, V. Strocov, Dariusz Gawryluk, Ekaterina Pomjakushina, K. Conder, Nicholas Plumb, Milan Radovic, Gabriel Autès, Oleg Yazyev, Zanxi Fang, Xianzhu Dai, Tan Qian, J. Mesot, Hanjie Ding, and Ming Shi, "Observation of weyl nodes and fermi arcs in tantalum phosphide," *Nature Communications* **7**, 11006 (2016).

¹⁹ Su-Yang Xu, Nasser Alidoust, Ilya Belopolski, Zhujun Yuan, Guang Bian, Tay-Rong Chang, Hao Zheng, Vladimir Strocov, Daniel Sanchez, Guoqing Chang, Chenglong Zhang, Daixiang Mou, Yun Wu, Lunan Huang, Chi-Cheng Lee, Shin-Ming Huang, Baokai Wang, Arun Bansil, Horng-Tay Jeng, and M. Zahid Hasan, "Discovery of a weyl fermion state with fermi arcs in niobium arsenide," *Nature Physics* **11**, 748–754 (2015).

²⁰ Qiang Li, Dmitri Kharzeev, Chuandi Zhang, Yuan Huang, Ivo Pletikosić, Alexei Fedorov, Ruidan Zhong, J.A. Schneeloch, G.D. Gu, and Tonica Valla, "Chiral magnetic effect in zrte5," *Nature Physics* **12** (2016), 10.1038/nphys3648.

²¹ P. Moll, Nityan Nair, Toni Helm, Andrew Potter, Itamar Kimchi, Ashvin Vishwanath, and James Analytis, "Transport evidence for fermi-arc-mediated chirality transfer in the dirac semimetal cd3as2," *Nature* **535** (2016), 10.1038/nature18276.

²² Ari Turner and Ashvin Vishwanath, "Beyond band insulators: Topology of semimetals and interacting phases," *Contemporary Concepts of Condensed Matter Science* **6**, 293–324 (2013).

²³ Chen Fang, Matthew J. Gilbert, Xi Dai, and B. Andrei Bernevig, "Multi-weyl topological semimetals stabilized by point group symmetry," *Phys. Rev. Lett.* **108**, 266802 (2012).

²⁴ Shin-Ming Huang, Su-Yang Xu, Ilya Belopolski, Chi-Cheng Lee, Guoqing Chang, Tay-Rong Chang, BaoKai Wang, Nasser Alidoust, Guang Bian, Madhab Neupane, Daniel Sanchez, Hao Zheng, Horng-Tay Jeng, Arun Bansil, Titus Neupert, Hsin Lin, and M. Zahid Hasan, "New type of weyl semimetal with quadratic double weyl fermions," *Proceedings of the National Academy of Sciences* **113**, 1180–1185 (2016).

²⁵ Seongjin Ahn, E. H. Hwang, and Hongki Min, "Collective modes in multi-weyl semimetals," *Scientific Reports* **6** (2016), 10.1038/srep34023.

²⁶ Hsin-Hua Lai, "Correlation effects in double-weyl semimetals," *Phys. Rev. B* **91**, 235131 (2015).

²⁷ Shao-Kai Jian and Hong Yao, "Correlated double-weyl semimetals with coulomb interactions: Possible applications to hgcr₂se₄ and srsi₂," *Phys. Rev. B* **92**, 045121 (2015).

²⁸ Huqing Huang, Zhirong Liu, Hongbin Zhang, Wenhui Duan, and David Vanderbilt, "Emergence of a chern-insulating state from a semi-dirac dispersion," *Phys. Rev. B* **92**, 161115 (2015).

²⁹ P. K. Pyatkovskiy and Tapash Chakraborty, "Dynamical polarization and plasmons in a two-dimensional system with merging dirac points," *Phys. Rev. B* **93**, 085145 (2016).

³⁰ Bahadur Singh, Guoqing Chang, Tay-Rong Chang, Shin-Ming Huang, Chenliang Su, Ming-Chieh Lin, Hsin Lin, and Arun Bansil, "Tunable double-weyl fermion semimetal state in the srsi₂ materials class," *Scientific Reports* **8**, 10540 (2018).

³¹ Tong Guan, Chaojing Lin, Chongli Yang, Youguo Shi, Cong Ren, Yongqing Li, Hongming Weng, Xi Dai, Zhong Fang, Shishen Yan, and Peng Xiong, "Evidence for half-metallicity in *n*-type hgcr₂se₄," *Phys. Rev. Lett.* **115**, 087002 (2015).

³² Ziming Zhu, Ying Liu, Zhi-Ming Yu, Shan-Shan Wang, Y. X. Zhao, Yuanping Feng, Xian-Lei Sheng, and

Shengyuan A. Yang, "Quadratic contact point semimetal: Theory and material realization," *Phys. Rev. B* **98**, 125104 (2018).

³³ Qihang Liu and Alex Zunger, "Predicted realization of cubic dirac fermion in quasi-one-dimensional transition-metal monochalcogenides," *Phys. Rev. X* **7**, 021019 (2017).

³⁴ Shuichi Murakami and Naoto Nagaosa, "Berry phase in magnetic superconductors," *Phys. Rev. Lett.* **90**, 057002 (2003).

³⁵ Tobias Meng and Leon Balents, "Weyl superconductors," *Phys. Rev. B* **86**, 054504 (2012).

³⁶ Gil Young Cho, Jens H. Bardarson, Yuan-Ming Lu, and Joel E. Moore, "Superconductivity of doped weyl semimetals: Finite-momentum pairing and electronic analog of the ³he-a phase," *Phys. Rev. B* **86**, 214514 (2012).

³⁷ Yi Li and F. D. M. Haldane, "Topological nodal cooper pairing in doped weyl metals," *Phys. Rev. Lett.* **120**, 067003 (2018).

³⁸ C. Sun, S.-P. Lee, and Y. Li, "Vortices in a monopole superconducting weyl semi-metal," *arXiv.1909.04179v2* (2020), 10.48550/arXiv.1909.04179.

³⁹ Enrique Muñoz, Rodrigo Soto-Garrido, and Vladimir Jurićć, "Monopole versus spherical harmonic superconductors: Topological repulsion, coexistence, and stability," *Phys. Rev. B* **102**, 195121 (2020).

⁴⁰ Enrique Muñoz, Juan Pablo Esparza, José Braun, and Rodrigo Soto-Garrido, "Topological versus conventional superconductivity in a Weyl semimetal: A microscopic approach," *Superconductivity* **12**, 100132 (2024).

⁴¹ Bitan Roy, Pallab Goswami, and Vladimir Jurićć, "Interacting weyl fermions: Phases, phase transitions, and global phase diagram," *Phys. Rev. B* **95**, 201102 (2017).

phase diagram," *Phys. Rev. B* **95**, 201102 (2017).

Appendix A: Green Function

From the Hamiltonian $\hat{H}_{BdG}(\mathbf{k})$, the finite temperature Green function in euclidean time satisfies

$$\left(\frac{\partial}{\partial \tau} + \hat{H}_{BdG}(\mathbf{k}) \right) \hat{G}_{\mathbf{k}}(\tau) = \delta(\tau), \quad (\text{A1})$$

written in Matsubara frequency space

$$\hat{G}_{\mathbf{k}}(\omega_n) = \int_0^\beta d\tau e^{i\omega_n \tau} \hat{G}_{\mathbf{k}}(\tau), \quad (\text{A2})$$

where $\omega_n = (2n + 1)\pi/\beta$, with $n \in \mathbb{Z}$ is the fermionic Matsubara frequency. In our model we calculate the finite temperature Green function by means

$$\hat{G}_{\mathbf{k}}(\omega_n) = \left[-i\omega_n + \hat{H}_{BdG}(\mathbf{k}) \right]^{-1}, \quad (\text{A3})$$

dividing the Green function in 2×2 matrix blocks, i.e.

$$\hat{G}_{\mathbf{k}}(\omega_n) = \begin{pmatrix} \hat{G}_{\mathbf{k}}^{\text{intra},-} & \hat{G}_{\mathbf{k}}^{\text{inter}} \\ (\hat{G}_{\mathbf{k}}^{\text{inter}})^\dagger & \hat{G}_{\mathbf{k}}^{\text{intra},+} \end{pmatrix}, \quad (\text{A4})$$

and inverting the 4×4 matrix $-i\omega_n + \hat{H}_{BdG}(\mathbf{k})$, we obtain

$$\hat{G}_{\mathbf{k}}^{\text{intra},\pm} = \frac{(E_{\mathbf{k}}^2 \pm \delta\mu\bar{\xi}_{\mathbf{k}}) [i\omega_n \hat{\eta}_0 + \xi_{\mathbf{k}}^\pm \hat{\eta}_3 + \Re \Delta_{\mathbf{k}}^{\text{intra}} \hat{\eta}_1 - \Im \Delta_{\mathbf{k}}^{\text{intra}} \hat{\eta}_2] \pm \delta\mu |\Delta_{\mathbf{k}}^{\text{inter}}|^2 \hat{\eta}_3 - 2B_{\mathbf{k}} (\Re \Delta_{\mathbf{k}}^{\text{inter}} \hat{\eta}_1 - \Im \Delta_{\mathbf{k}}^{\text{inter}} \hat{\eta}_2)}{E_{\mathbf{k}}^4 - 4B_{\mathbf{k}}^2 - \delta\mu^2 (\bar{\xi}_{\mathbf{k}}^2 + |\Delta_{\mathbf{k}}^{\text{inter}}|^2)}, \quad (\text{A5})$$

$$\begin{aligned} \hat{G}_{\mathbf{k}}^{\text{inter}} = & \frac{-2B_{\mathbf{k}} \left[\left(i\omega_n + \frac{\delta\mu}{2} \right) \hat{\eta}_0 + \bar{\xi}_{\mathbf{k}} \hat{\eta}_3 + \Re \Delta_{\mathbf{k}}^{\text{intra}} \hat{\eta}_1 - \Im \Delta_{\mathbf{k}}^{\text{intra}} \hat{\eta}_2 \right] + \delta\mu \Delta_{\mathbf{k}}^{\text{intra}} (\Delta_{\mathbf{k}}^{\text{inter}})^* \hat{\eta}_0}{E_{\mathbf{k}}^4 - 4B_{\mathbf{k}}^2 - \delta\mu^2 (\bar{\xi}_{\mathbf{k}}^2 + |\Delta_{\mathbf{k}}^{\text{inter}}|^2)} \\ & + \frac{\left(E_{\mathbf{k}}^2 - \frac{\delta\mu^2}{2} \right) (\Re \Delta_{\mathbf{k}}^{\text{inter}} \hat{\eta}_1 - \Im \Delta_{\mathbf{k}}^{\text{inter}} \hat{\eta}_2) + \omega_n \delta\mu (\Im \Delta_{\mathbf{k}}^{\text{inter}} \hat{\eta}_1 + \Re \Delta_{\mathbf{k}}^{\text{inter}} \hat{\eta}_2)}{E_{\mathbf{k}}^4 - 4B_{\mathbf{k}}^2 - \delta\mu^2 (\bar{\xi}_{\mathbf{k}}^2 + |\Delta_{\mathbf{k}}^{\text{inter}}|^2)}, \end{aligned} \quad (\text{A6})$$

where $(\cdot)^\dagger$ is the conjugate transpose, considering $(i\omega_n)^* = i\omega_n$.

Appendix B: Gap Equations

From the matrix elements of Green Function we obtain the following correlation functions

$$\begin{aligned} \langle \hat{\alpha}_-(\mathbf{k}) \hat{\alpha}_-(-\mathbf{k}) \rangle &= [\hat{G}_{\mathbf{k}}^{\text{intra},-}]_{12} \quad (\text{B1}) \\ &= \frac{\Delta_{\mathbf{k}}^{\text{intra}} (E_{\mathbf{k}}^2 - \delta\mu\bar{\xi}_{\mathbf{k}}) - 2\Delta_{\mathbf{k}}^{\text{inter}} B_{\mathbf{k}}}{E_{\mathbf{k}}^4 - 4B_{\mathbf{k}}^2 - \delta\mu^2 (\bar{\xi}_{\mathbf{k}}^2 + |\Delta_{\mathbf{k}}^{\text{inter}}|^2)}, \end{aligned}$$

$$\begin{aligned} \langle \hat{\alpha}_-(\mathbf{k}) \hat{\alpha}_+(-\mathbf{k}) \rangle &= [\hat{G}_{\mathbf{k}}^{\text{inter}}]_{12} \quad (\text{B2}) \\ &= \frac{\Delta_{\mathbf{k}}^{\text{inter}} (E_{\mathbf{k}}^2 - \frac{\delta\mu^2}{2}) - 2\Delta_{\mathbf{k}}^{\text{intra}} B_{\mathbf{k}} - i\omega_n \delta\mu \Delta_{\mathbf{k}}^{\text{inter}}}{E_{\mathbf{k}}^4 - 4B_{\mathbf{k}}^2 - \delta\mu^2 (\bar{\xi}_{\mathbf{k}}^2 + |\Delta_{\mathbf{k}}^{\text{inter}}|^2)}. \end{aligned}$$

Substituting in the following gap equations

$$\Delta_{\mathbf{k}}^{\text{intra}} = T \sum_{\mathbf{k}', \omega_n} V_{\text{intra}}(\mathbf{k}, \mathbf{k}') \langle \hat{\alpha}_-(\mathbf{k}') \hat{\alpha}_-(-\mathbf{k}') \rangle, \quad (\text{B3})$$

$$\Delta_{\mathbf{k}}^{\text{inter}} = T \sum_{\mathbf{k}', \omega_n} V_{\text{inter}}(\mathbf{k}, \mathbf{k}') \langle \hat{\alpha}_-(\mathbf{k}') \hat{\alpha}_+(-\mathbf{k}') \rangle, \quad (\text{B4})$$

we obtain

$$\Delta_{\mathbf{k}}^{\text{intra}} = T \sum_{\mathbf{k}', \omega_n} V_{\text{intra}}(\mathbf{k}, \mathbf{k}') \frac{\Delta_{\mathbf{k}'}^{\text{intra}} (E_{\mathbf{k}'}^2 - \delta\mu\bar{\xi}_{\mathbf{k}'}) - 2\Delta_{\mathbf{k}'}^{\text{inter}} B_{\mathbf{k}'}}{E_{\mathbf{k}'}^4 - 4B_{\mathbf{k}'}^2 - \delta\mu^2 (\bar{\xi}_{\mathbf{k}'}^2 + |\Delta_{\mathbf{k}'}^{\text{inter}}|^2)} \quad (\text{B5})$$

$$\Delta_{\mathbf{k}}^{\text{inter}} = T \sum_{\mathbf{k}', \omega_n} V_{\text{inter}}(\mathbf{k}, \mathbf{k}') \frac{\Delta_{\mathbf{k}'}^{\text{inter}}(E_{\mathbf{k}'}^2 - \frac{\delta\mu^2}{2}) - 2\Delta_{\mathbf{k}'}^{\text{intra}} B_{\mathbf{k}'}}{E_{\mathbf{k}'}^4 - 4B_{\mathbf{k}'}^2 - \delta\mu^2(\bar{\xi}_{\mathbf{k}'}^2 + |\Delta_{\mathbf{k}'}^{\text{inter}}|^2)} \text{ so the denominator of both gap equations can be written}$$

$$(B6)$$

where the term proportional to $i\omega_n$ was eliminated in the last equation, since it vanishes when adding in ω_n . Then, we define

$$\begin{aligned} \Gamma_{\mathbf{k}}^2 &= \bar{\xi}_{\mathbf{k}}^2 + |\Delta_{\mathbf{k}}^{\text{intra}}|^2 + |\Delta_{\mathbf{k}}^{\text{inter}}|^2 + \frac{\delta\mu^2}{4} \\ &+ \sqrt{4B_{\mathbf{k}}^2 + \delta\mu^2(\bar{\xi}_{\mathbf{k}}^2 + |\Delta_{\mathbf{k}}^{\text{inter}}|^2)}, \end{aligned} \quad (B7)$$

$$E_{\mathbf{k}}^4 - 4B_{\mathbf{k}}^2 - \delta\mu^2(\bar{\xi}_{\mathbf{k}}^2 + |\Delta_{\mathbf{k}}^{\text{inter}}|^2) = (\omega_n^2 + \Gamma_{\mathbf{k}}^2)(\omega_n^2 + \gamma_{\mathbf{k}}^2), \quad (B9)$$

$$\begin{aligned} \gamma_{\mathbf{k}}^2 &= \bar{\xi}_{\mathbf{k}}^2 + |\Delta_{\mathbf{k}}^{\text{intra}}|^2 + |\Delta_{\mathbf{k}}^{\text{inter}}|^2 + \frac{\delta\mu^2}{4} \\ &- \sqrt{4B_{\mathbf{k}}^2 + \delta\mu^2(\bar{\xi}_{\mathbf{k}}^2 + |\Delta_{\mathbf{k}}^{\text{inter}}|^2)}, \end{aligned} \quad (B8)$$

and we perform the decomposition into partial fractions to obtain

$$\begin{aligned} \Delta_{\mathbf{k}}^{\text{intra}} &= \frac{T}{2} \sum_{\mathbf{k}', \omega_n} V_{\text{intra}}(\mathbf{k}, \mathbf{k}') \left[\left(\Delta_{\mathbf{k}'}^{\text{intra}} + \frac{2\Delta_{\mathbf{k}'}^{\text{inter}} B_{\mathbf{k}'} + \delta\mu \bar{\xi}_{\mathbf{k}'} \Delta_{\mathbf{k}'}^{\text{intra}}}{\sqrt{4B_{\mathbf{k}'}^2 + \delta\mu^2(\bar{\xi}_{\mathbf{k}'}^2 + |\Delta_{\mathbf{k}'}^{\text{inter}}|^2)}} \right) \frac{1}{\omega_n^2 + \Gamma_{\mathbf{k}'}^2} \right. \\ &\left. + \left(\Delta_{\mathbf{k}'}^{\text{intra}} - \frac{2\Delta_{\mathbf{k}'}^{\text{inter}} B_{\mathbf{k}'} + \delta\mu \bar{\xi}_{\mathbf{k}'} \Delta_{\mathbf{k}'}^{\text{intra}}}{\sqrt{4B_{\mathbf{k}'}^2 + \delta\mu^2(\bar{\xi}_{\mathbf{k}'}^2 + |\Delta_{\mathbf{k}'}^{\text{inter}}|^2)}} \right) \frac{1}{\omega_n^2 + \gamma_{\mathbf{k}'}^2} \right], \end{aligned} \quad (B10)$$

$$\begin{aligned} \Delta_{\mathbf{k}}^{\text{inter}} &= \frac{T}{2} \sum_{\mathbf{k}', \omega_n} V_{\text{inter}}(\mathbf{k}, \mathbf{k}') \left[\left(\Delta_{\mathbf{k}'}^{\text{inter}} + \frac{2\Delta_{\mathbf{k}'}^{\text{intra}} B_{\mathbf{k}'} + \frac{\delta\mu^2}{2} \Delta_{\mathbf{k}'}^{\text{inter}}}{\sqrt{4B_{\mathbf{k}'}^2 + \delta\mu^2(\bar{\xi}_{\mathbf{k}'}^2 + |\Delta_{\mathbf{k}'}^{\text{inter}}|^2)}} \right) \frac{1}{\omega_n^2 + \Gamma_{\mathbf{k}'}^2} \right. \\ &\left. + \left(\Delta_{\mathbf{k}'}^{\text{inter}} - \frac{2\Delta_{\mathbf{k}'}^{\text{intra}} B_{\mathbf{k}'} + \frac{\delta\mu^2}{2} \Delta_{\mathbf{k}'}^{\text{inter}}}{\sqrt{4B_{\mathbf{k}'}^2 + \delta\mu^2(\bar{\xi}_{\mathbf{k}'}^2 + |\Delta_{\mathbf{k}'}^{\text{inter}}|^2)}} \right) \frac{1}{\omega_n^2 + \gamma_{\mathbf{k}'}^2} \right]. \end{aligned} \quad (B11)$$

Finally, we use the identity

$$T \sum_{\omega_n} \frac{1}{\omega_n^2 + c^2} = \frac{\tanh\left(\frac{c}{2T}\right)}{c}, \quad (B12)$$

to obtain the gap equations of section III.

we define the following density of states function

$$\begin{aligned} \rho(\xi) &\equiv \int \frac{d^3 k}{(2\pi)^3} \delta(\xi - \xi_{\mathbf{k}}) \\ &= \int \frac{d^3 k}{(2\pi)^3} \delta\left(\xi + \mu - v_f \sqrt{k_z^2 + \alpha^2 k_{\perp}^{2\nu}}\right) \\ &= \frac{1}{(2\pi)^2 v_f} \left(\frac{\xi + \mu}{\alpha v_f}\right)^{2/\nu} \frac{\beta(\frac{1}{\nu}, \frac{1}{2})}{\nu}. \end{aligned} \quad (C2)$$

Then

$$\int \frac{d^3 k}{(2\pi)^3} f(\Omega_{\mathbf{k}}, \xi_{\mathbf{k}}) = \int_{-\omega_D}^{\omega_D} d\xi \int \frac{d^3 k}{(2\pi)^3} \delta(\xi - \xi_{\mathbf{k}}) f(\Omega_{\mathbf{k}}, \xi). \quad (C3)$$

Using cylindrical coordinates $d^3 k = k_{\perp} dk_{\perp} d\phi dk_z$, we use the properties of the δ function to solve the integral in dk_z , and then we make the change of variable $x = \left(\frac{\alpha v_f}{\xi + \mu}\right)^{1/\nu} k_{\perp}$ to obtain

$$\sum_{\mathbf{k}} f(\Omega_{\mathbf{k}}, \xi_{\mathbf{k}}) \approx \int \frac{d^3 k}{(2\pi)^3} f(\Omega_{\mathbf{k}}, \xi_{\mathbf{k}}), \quad (C1)$$

To take continuous limit of the form

$$\sum_{\mathbf{k}} f(\Omega_{\mathbf{k}}, \xi_{\mathbf{k}}) \approx \int \frac{d^3 k}{(2\pi)^3} f(\Omega_{\mathbf{k}}, \xi_{\mathbf{k}}), \quad (C1)$$

$$\begin{aligned}
\int \frac{d^3k}{(2\pi)^3} f(\Omega_{\mathbf{k}}, \bar{\xi}_{\mathbf{k}}) &= 2 \int_{-\omega_D}^{\omega_D} \frac{d\xi}{(2\pi)^2 v_f} \left(\frac{\xi + \mu}{\alpha v_f} \right)^{2/\nu} \int_0^1 \frac{dx x}{\sqrt{1 - x^{2\nu}}} \int_0^{2\pi} \frac{d\phi}{2\pi} f(\theta_x, \phi, \xi) \\
&= \frac{2\nu}{\beta(\frac{1}{\nu}, \frac{1}{2})} \int_{-\omega_D}^{\omega_D} d\xi \rho(\xi) \int_0^1 \frac{dx x}{\sqrt{1 - x^{2\nu}}} \int_0^{2\pi} \frac{d\phi}{2\pi} f(\theta_x, \phi, \xi),
\end{aligned} \tag{C4}$$

where θ_x is defined by

$$\tan \theta_x = \frac{cx}{\sqrt{1 - x^{2\nu}}}, \tag{C5}$$

with

$$c = \alpha^{-1/\nu} \left(\frac{\xi + \mu}{v_f} \right)^{\frac{1}{\nu} - 1} \approx \alpha^{-1/\nu} \left(\frac{\mu}{v_f} \right)^{\frac{1}{\nu} - 1}. \tag{C6}$$

We make the approximation of evaluating $\rho(\xi)$ at $\xi = 0$, since the density of states is centered at that value. Finally the integral remains

$$\int \frac{d^3k}{(2\pi)^3} f(\Omega_{\mathbf{k}}, \bar{\xi}_{\mathbf{k}}) = \frac{\rho(0)}{B_\nu} \int_0^1 \frac{dx x}{\sqrt{1 - x^{2\nu}}} \int_0^{2\pi} \frac{d\phi}{2\pi} \int_{-\omega_D}^{\omega_D} d\xi f(\theta_x, \phi, \xi), \tag{C7}$$

with $B_\nu = \beta(\frac{1}{\nu}, \frac{1}{2})/(2\nu)$